MATHIAS ALTEN
SUPERVISOR: OVE MIKKELSEN

Design of Upright

For ION racing

Bachelor thesis 2024

Mechanical engineering

Department of Mechanical and Structural Engineering and Material science

Faculty of science and technology

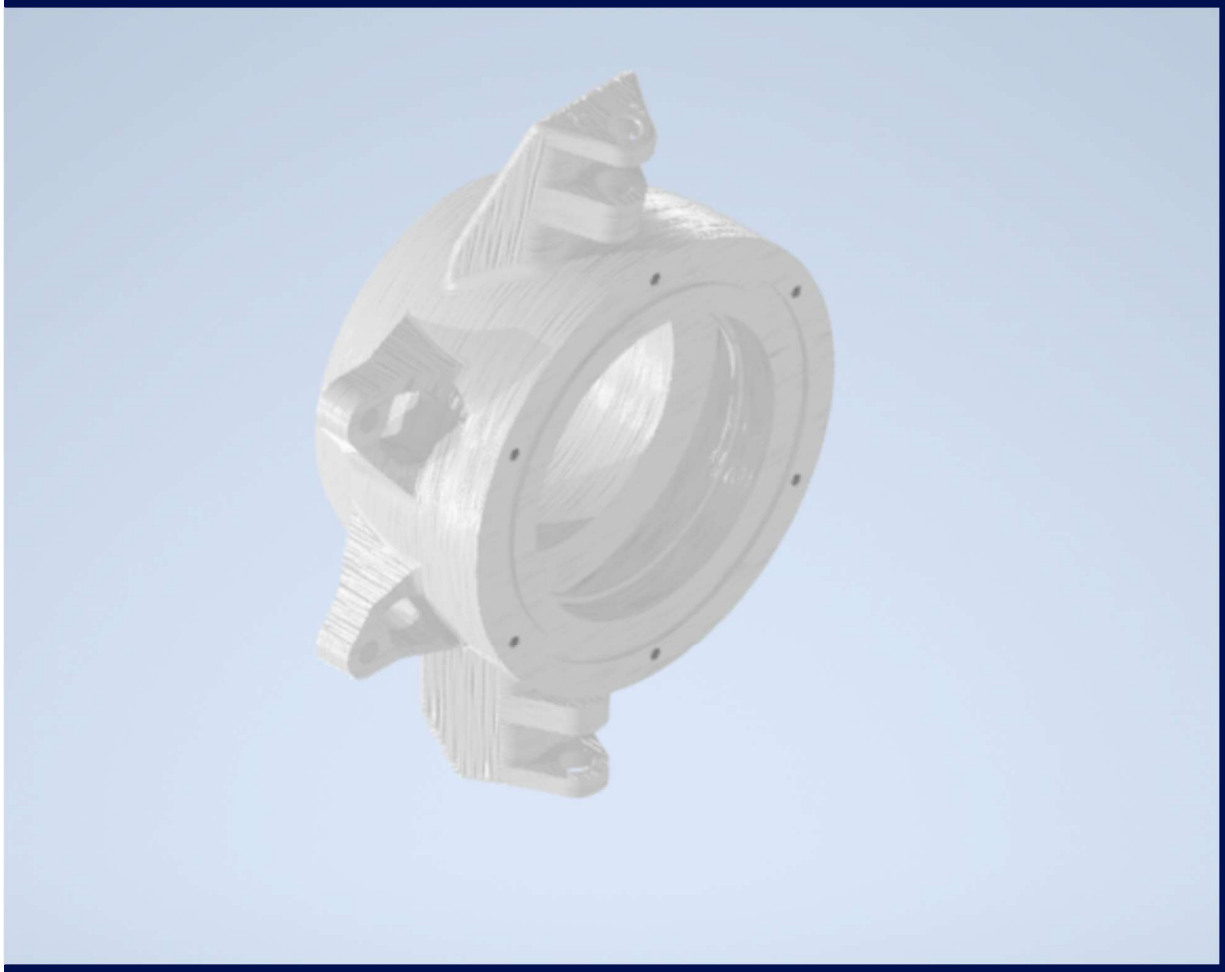

Foreword

This thesis represents the culmination of a two-year journey with ION Racing. My engagement with this project encapsulates the essence of this experience. The focused determination, nurturing atmosphere of creativity, and unwavering commitment fostered during my time with ION Racing have positively shaped me. I am deeply thankful for the opportunities provided by the organisation and the support of its members.

In closing, I extend my appreciation to both the current and previous ION Racing teams for providing me with the knowledge upon which this thesis is built further on. A special acknowledgement goes to Steven Høiland for his substantial contributions to the prior calculations utilized in this thesis. Additionally, I express my sincere gratitude to my supervisor, Ove Mikkelsen, for his guidance throughout this project.

Abstract

This thesis, conducted for ION Racing, focuses on the development of a four-wheel drive transmission system for a Formula Student race car. The system employs four electric motors to deliver power to all four wheels, aiming to optimize performance and efficiency. Where this thesis focuses on the biggest parts, the uprights. This was done with computer-aided design and simulation in Autodesk Inventor. Firstly, the requirements for the design were set, before multiple concept designs were made, and one was selected for further development. The main differences being the possible manufacturing method and the different possibilities these methods lead to. The evaluation of results demonstrates that this design is a viable option for ION Racing's future conversions. This conventional design has been produced using traditional manufacturing methods, indicating its practicality and feasibility for implementation.

Table of Contents

1. Introduction

1.1 Project background

1.1.1 Formula Student

Formula Student is an international student competition that takes place in various parts of the world, including the United Kingdom, the USA, Finland, and Germany. The competition in the United Kingdom is organized by IMechE with the aim of engaging and encouraging students to pursue a career in engineering. The competition challenges students in design, manufacturing, and collaboration through the construction of a single-seater race car to compete in the event. In addition to the technical aspects of building a car, students are also challenged in areas such as marketing, cost reports, design presentations, and scrutineering in front of a panel of judges. Through this competition, students have a valuable and unique opportunity to develop and acquire new knowledge and put it into practice. ION Racing will participate in this year's competition, taking place at the Silverstone Circuit in the UK.

1.1.2 ION Racing

ION Racing is a student organization that was formed in 2011, originally consisting primarily of mechanical engineers. Since then, the team has grown larger every year and now comprises nearly fifty participants, including students from mechanical and electrical engineering, as well as computer science, marketing, and economics backgrounds. Since 2014, the team’s car has been electric with one motor powering the back wheels; in other words, it is rear wheel drive. However, as the knowledge and quality of the team has grown it has outgrown this design. Therefore, the team wants to convert to four-wheel drive with motors on all four wheels. This is just one of the many projects the team is working on to continually improve the car.

1.2 Project goals

The goal of this project is therefore to design a wheel assembly that makes it possible for ION racing to convert to four-wheel drive in the future. However, this project is much bigger than this bachelor thesis and consists of two other thesis that are worked on simultaneously at ION Racing. This thesis will therefore only focus on the design of the new front and rear uprights. This is the part connecting the motor, wheel hub, and tie rods. The old design that ION racing used can be observed in Figure 2.1.3.

1.2.1 Requirements

Measurable requirements for the design were established to ensure that the objectives could be achieved and verified. These requirements for the upright are divided into hard and soft requirements. The hard requirements are of the utmost importance, and failure to meet them would result in the design being deemed unsuccessful, while the soft requirements are desirable but not necessary. This division can be seen below.

Hard requirements

- The design needs to comply with the FSUK 2024 rules.
- The design must be able to manage the forces it experiences.
- The design must fit together with the rest of the 4-wheel drive transmission system under development simultaneously at ION Racing.
- The design must be possible to manufacture, both with regards to ION Racing's finances and its available manufacturing techniques.

Soft requirements

- The design must be as future-proof as possible.
- The design must be lighter or the same weight as the previous generation.

2. Literature and methodology

Before diving into the development of the new upright, it is first important to gather some fundamental understanding of the theory used in the development process.

2.1 The wheel assembly

Figure 2.1.1 Shows an example wheel assembly from a formula student car (grabcad.com, 2024).

The upright serves as the main structure in a suspension system, with the task of transferring all forces acting on each wheel to the suspension arms and damping system, and further into the chassis. Additionally, an upright function as a housing for the wheel bearings and hub, enabling the wheel to rotate. It securely holds the brake callipers in place, thus absorbing the reaction forces between the brake disc and callipers during braking. Moreover, it acts as a linkage between the upper and lower suspension arms. In Figure 2.1.1 below one can see an example of a wheel assembly. Here one clearly sees how it connects all parts of the wheel system. The top and bottom poles in the picture are named control arms. Control arms, also known as A-arms or wishbones, are structural components that connect the wheel hub to the chassis of the vehicle through the upright. They come in various shapes and designs, depending on the vehicle's design and performance requirements (Tsyauto, 2024).

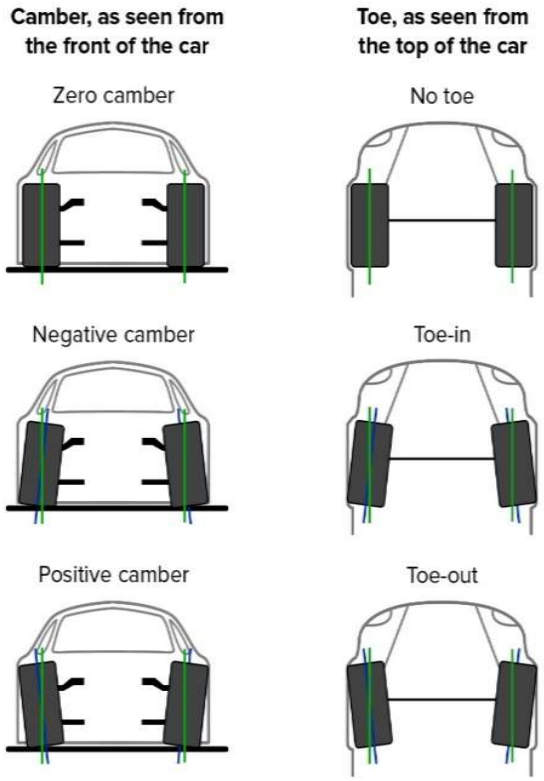

Figure 2.1.2 Illustrates what camber and toe is (Krönke, 2024).

The performance of the car can also be adjusted using the upright by changing the camber, toe and caster angle. In Figure 2.1.1, one can see that the upper control arm can be angled by the upright. This adjustment creates a camber for the wheel. Figure 2.1.2. clearly illustrates what is meant by camber and toe. This affects how the car is controlled, no more will be said about that in this thesis other than it can be controlled by the design of the upright.

In Figure 2.1.3 one can see that ION racing previously used an upright design where one could adjust the chamber by adding shims. This made the design very flexible. However, it is heavy and not on par with ION racing's increased focus on weight reduction.

Figure 2.1.3 Picture of previously used up-right by ION-racing. This design was basic but effective. As well as being flexible. However, due to changing criteria from ION racing it is no longer suitable.

In the previous design shown in Figure 2.1.3 on the left of the upright one can see a bracket for mounting the break. This can also be seen in red in Figure 2.1.1. This is where the break force acts, which is the biggest force. Thus, it must be strong.

2.2 Unsprung and sprung weight

The mass of a car can be divided into two parts, the unsprung and the sprung weight. The sprung weight is the weight of the car that is dampened by the suspension, while the unsprung weight is the weight that is not dampened by the suspension. An illustration of this is shown in Figure 2.2.1.

The unsprung weight of a vehicle plays a pivotal role in influencing the driving experience. It directly impacts the vehicle's handling, responsiveness, and overall feel on the road. Understanding and optimizing the unsprung weight is essential for enhancing vehicle performance and ensuring a satisfying driving experience for the users. The smaller the amount of unsprung weight, the more effective the suspension will be. Consequently, the more efficient the suspension is the more grip the tires have. Therefore, reducing the unsprung weight will result in an overall better handling vehicle with a better driving feel while an increase will negatively affect these aspects (Valor Offroad, 2024).

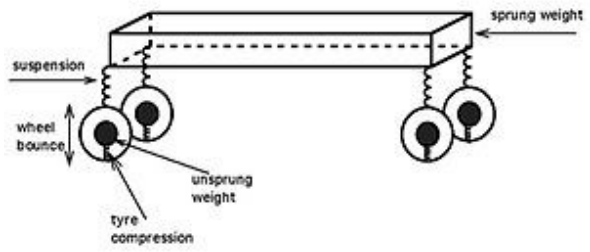

Figure 2.2.1 illustrates what unsprung and sprung weight is. This is important because this is greatly affected by the design of the upright (Ingham, 2024).

The unsprung weight usually includes the suspension, brakes, upright, wheels and tires. However, ION racing wants to have motors on all four wheels, which means that the motors would also contribute to the unsprung weight. For this reason, it is especially important for ION racing to minimize the weight of the other parts, to mitigate the undesirable effects of the added unsprung weight (Valor Offroad, 2024).

2.3 Computer-aided design and simulation

Computer-aided design, more commonly known as CAD, has emerged as an indispensable tool across various industries, revolutionizing the way designers and engineers conceptualize, develop, and refine their creations. CAD makes it possible to visualize a design faster and better than before. This is achieved by developing designs, sketching, and

producing technical drawings, instead of doing this manually. In the development of an upright, this is beneficial. An example of a CAD design can be observed in Figure 2.3.1.

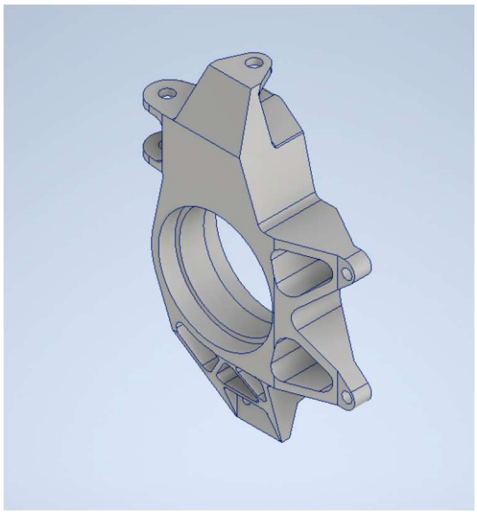

Figure 2.3.1 illustrates example CAD design. This example is the previous upright design used by ION Racing.

In addition to digital modelling, it is also possible to simulate how the part will behave in different situations. This simulation provides a visual representation showing where the highest stresses are and their magnitude. As shown in Figure 2.3.2, the colour bar on the left side of the image indicates that the maximum stress is 320 MPa. This technology allows for faster identification of maximum stress, especially in complex geometries that would otherwise be difficult to analyse.

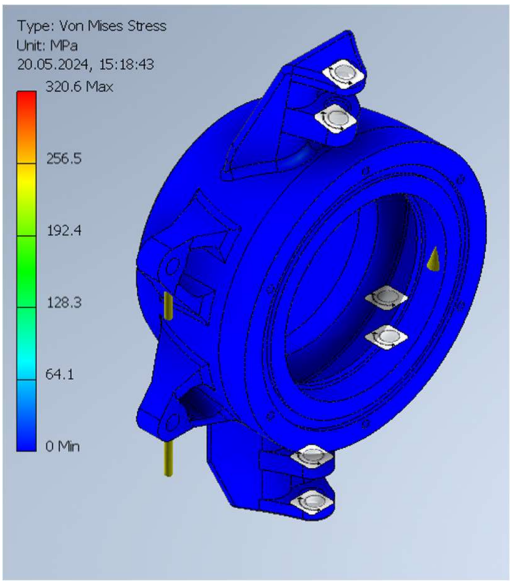

Figure 2.3.2 illustrates an example result from a simulation. With the stress displayed in the bar on the left and where the stress is given on the figure.

In Figure 2.3.3, a typical convergence curve and the reason for the change in simulated stresses can be observed. The figure illustrates that a smaller mesh size increases the accuracy of the simulated stresses. However, the increase in accuracy per decrease in mesh size converges and eventually becomes minimal. Since simulations take exponentially longer with smaller mesh sizes, it is desirable to use the largest possible mesh size that still provides an accurate simulation (Nafems, 2024).

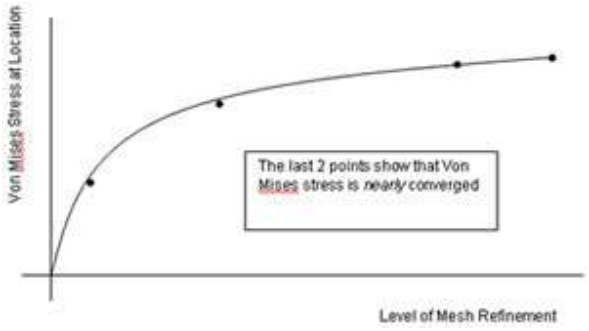

Figure 2.3.3 illustrates the convergence curve for changing mesh size. One can observe that the accuracy increases with the increase of level of mesh refinement. However, the increase converges and at a point it is not worth it to increase the level in the mesh refinement more (Nafems, 2024).

In Figure 2.3.4, one can see a representation of a mesh on the upright. It is a grid of cells dividing the object into small parts called elements. This division allows computers to simulate the behaviour of the object by solving partial differential equations over complex objects using numerical methods. This approach is utilized in both computer-aided design and the finite element method (Massobrio, 2024).

Figure 2.3.4 illustrates the upright part with mesh. The black lines over the part are the mesh. This is the Upright in the concept development of this project and the mesh is used in the simulation at that stage.

To enhance weight reduction in the design, Autodesk Inventor's shape generator function can be utilized. This tool simplifies identifying unnecessary components, thereby optimizing the overall design. Figure 2.3.5 illustrates the results of a shape generator simulation conducted using Autodesk Inventor.

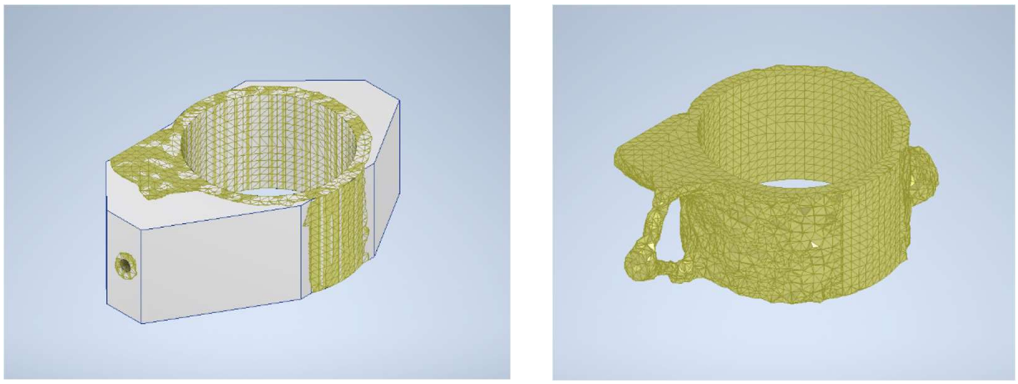

(a) (b)

Figure 2.3.5 illustrates results from a simulation in CAD and how it helps the engineer to optimize the design. Part (a) illustrates the block given to simulate where some parameters are set for what must be kept the same and what can be changed. In part (b) one can see the design suggested after performing a shape generator simulation and removing unnecessary mass. This is used to make the design lighter and thus better.

This is a suggestion made by Inventor on which material can be subtracted based on where the biggest stresses are. Note that this is only a suggestion, and experience is still necessary. Using this suggestion, one can remove some material and then perform a new stress analysis simulation to ensure the design can still handle the experienced stresses. However, one can see in Figure 2.3.5 that this often generates complicated shapes which are not possible to manufacture using traditional manufacturing methods. Instead, one would need to use additive manufacturing, which is discussed in more detail in chapter 2.4.

The function shape generator is used by first generating a block, as shown in Figure 2.3.5.(a). After this, the design requirements are set. In this example, these are the dimensions of the hub, the mounting points, and the required material around them. In addition, the forces and their directions are added. Lastly, the constraints are set. Then the simulation can be performed, where one decides by what percentage the weight should be reduced (Autodesk Inventor, 2024).

2.4 Manufacturing methods

There are multiple ways to manufacture an upright. The traditional method, and how it previously has been done at ION Racing, is subtractive manufacturing. This method limits what designs are possible. However, for simple designs, it is often the best option due to its relative simplicity, allowing the students at ION Racing to do it themselves.

A new and increasingly popular method is additive manufacturing, also known as 3D printing. This makes it possible to manufacture significantly more complex designs. However, the drawback of this method is that the strength of the material can be compromised. It is also significantly more complex and requires more knowledge to perform than traditional manufacturing methods. Additionally, additive manufacturing is significantly more expensive, and ION would rely on outsourcing the manufacturing.

(a) *(b)*

Figure 2.4.1 illustrates the difference in possibilities between additive manufacturing in part a on the left and traditional machining on the right in Figure (b). Figure (a) is a complex organic shape which would not be able to produce with traditional manufacturing because the tools would not get access to all the mass that must be removed. In contrast, Figure (b) has straight edges and is therefore possible to manufacture by subtracting the unnecessary mass (In3dtec, 2024) (In3dtec, 2024).

Figure 2.4.1 above shows why this might still be worth it for ION Racing. The design on the left shows a complex structure that only includes the absolute necessary material to minimize weight. The part almost looks like it was shaped by nature, which has evolved over millions of years. This is what digital analysis and simulations, combined with this production method, can achieve. In addition to removing unnecessary material as illustrated in Figure 2.4.1, one can also make the part lighter by removing material where a certain thickness is required. In ION Racing's case, there are several examples of this, one being the centre hub. Here, a lighter design could be obtained by having a lighter core. Figure 2.4.2 is an example of how this was done at Revolve NTNU (Aune, 2016) (In3dtec, 2024).

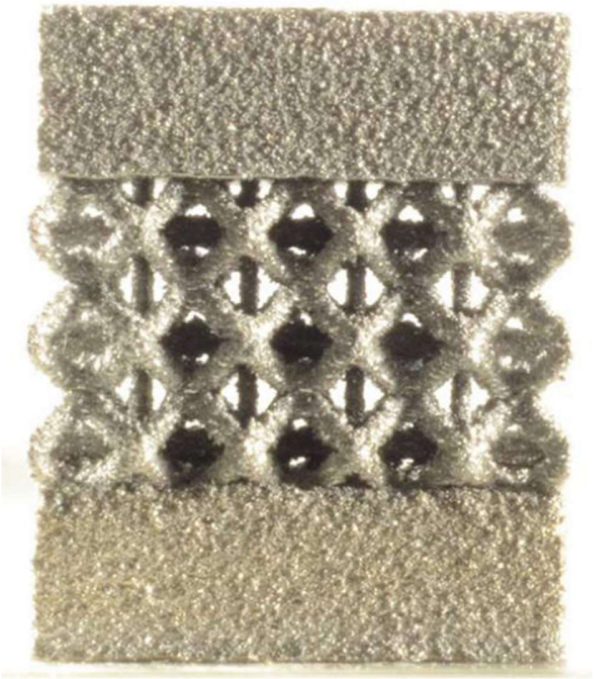

Figure 2.4.2 illustrates how additive manufacturing van be used to create a hollow core to minimize the material and thus weight. This example is form NTNU Revolve used on their upright (Aune, 2016).

2.5 Material properties

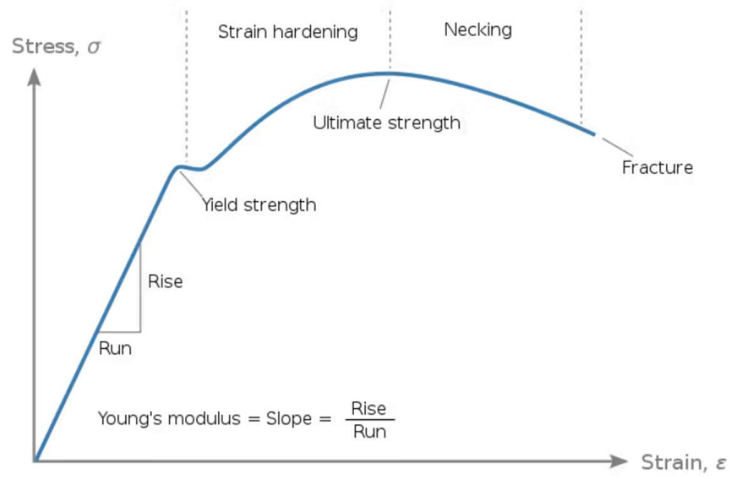

Figure 2.5.1 illustrates strain stress curve often used to measure the capabilities of a material. The curve illustrates how much the material strains with the increase in stress at different stages. One can also observe the definition of Young's modulus, Yield strength, Ultimate strength and fracture (Team Xometry, 2024).

Figure 2.5.1 shows a strain stress curve. This is often used to illustrate measurements of the strength of a material. In this context, the most important is the yield strength. This is the maximum stress before the deformation becomes plastic. Meaning permanent and that the deformation will not go back when the force is removed. This is undesirable; therefore, the design must be made so that the stresses are below this (Team Xometry, 2024).

This varies with materials and alloys. A commonly used material in this context is aluminium. Some alloys with suitable properties of this material are the alloys aluminium 2024 and aluminium 7075. These alloys have yield strengths of 324 MPa and 503 MPa (asm.matweb, 2024)

With the densities of the alloys is almost the same for both the alloys. Aluminium 2024 weighing 2.78 g/cc and aluminium 7075 2.81 g/cc. Thus Al 7075 has a significantly bigger specific yield strength. This is the yield strength per weight.

2.6 Product development

The product development process is a series of steps from an input problem needing a solution to a finished product. This is commonly divided into planning, concept development, system-level design, detail design, testing and refinement, and production ramp-up. ION racing had already done the planning of this project before it was given to me, so that is not relevant to this thesis. This project only focuses on the concept development, system-level design, and detail design. The testing, refinement, and product ramp-up will be done when the leaders in ION decide whether the project is worth going further with.

During concept development, the requirements and possibilities of the design are selected. In this context, these are the previously given requirements for the design. The possibilities include, for instance, the various manufacturing methods available. To identify the most possibilities, a multitude of different ideas must be generated. There are numerous strategies to come up with different ideas. A typical starting point is to look at what has been done already. However, it is different for everyone what works for them, so regardless of the method used to generate ideas, sketches are usually made. This may also help in generating more ideas (Ulrich, Eppinger, & Yang, 2020).

The system-level design in this case includes the definition of the product architecture; this means the geometric layout of the project. As the development of the Upright is a part of the bigger project of developing a new wheel assembly system, it is also determined by new criteria established by this project's geometric layout. The possible geometric layout is also determined by the chosen manufacturing method in the system-level design. After this, the only remaining task is to make final adjustments to optimize the design (Ulrich, Eppinger, & Yang, 2020).

The detailed design is the final part of the design process that this thesis includes. It encompasses the complete specification of the geometry, materials, and tolerances for the part. After this part of the design process, one should have all the necessary information to manufacture the part (Ulrich, Eppinger, & Yang, 2020).

3. Concept development and selection

The concept development revolved around selecting the type of design, including material, manufacturing method, and rough design. The focus was on two main concept designs: a simpler design that could be manufactured using traditional methods, and a design that needed to be manufactured using additive manufacturing, commonly known as 3D printing.

3.2 Material choice

Firstly, the material was selected. It is possible to make the upright from a variety of different materials; however, it is typically made from an aluminium alloy or titanium. Two examples of aluminium alloys are aerospace-grade alloys Al 2024 and Al 7075. To select the right material for ION Racing, the different strengths and weaknesses of these materials had to be compared. The parameters selected for comparison were the specific yield strength of the material, the feasibility of additive manufacturing, and material cost.

The specific yield strength of the material was considered to maximize the performance of the car by minimizing its weight. Given that adding weight to the wheel, such as in the upright, would make the car harder to steer, it is crucial to keep the weight down. In Chapter 2.5, the material properties of Al 2024 and Al 7075 are discussed. This analysis shows that Al 7075 has a higher yield strength. Additionally, using the same material for other parts by ION Racing could lead to advantages in purchasing and manufacturing the part. Therefore, it was decided to use Al 7075 which is already in use by ION Racing. All simulations from this point onward were conducted for that material and alloy.

3.1 Start point

The concept development begins with several predefined constraints, including designated points for bracket placement and specific inner dimensions. However, these parameters underwent changes throughout the design process due to the simultaneous development of the entire wheel assembly. Consequently, the design required multiple iterations and modifications. Table 3.1.1 illustrates the initial bracket points for the front left upright.

Table 3.1.1 shows the first given points for the brackets on the upright, where "UPRI" is an abbreviation for upright. The point "UPRI_LowPnt" is, therefore, the coordinate of the centre for the lowest bracket. From this point, mounting points for the bolts are needed in the correct direction at a distance of 8 mm. The same is the case for the upper point "UPRI_UppPnt" and the tie point for steering in the front and stabilizing the wheel in the back, named "UPRI_TiePnt".

	Point Name	Left		
		X	Y	Z
Double A-Arm	CHAS_LowFor	152,315	216,680	170,413
	CHAS_LowAft	-131,499	217,063	170,413
	CHAS_UppFor	139,369	265,086	277,621
	CHAS_UppAft	-122,423	267,015	277,621
	UPRI_LowPnt	5,000	549,000	150,000
	UPRI_UppPnt	-8,000	522,000	344,000
	CHAS_TiePnt	52,000	200,000	180,000
	UPRI_TiePnt	54,000	573,000	193,400

A table with the final points can be obtained from Appendix C. The original points shown in Table 3.1.1 were entered into Inventor. Since the design was created from scratch, multiple different concepts were developed. Figures 3.1.1 and 3.1.2 illustrate these.

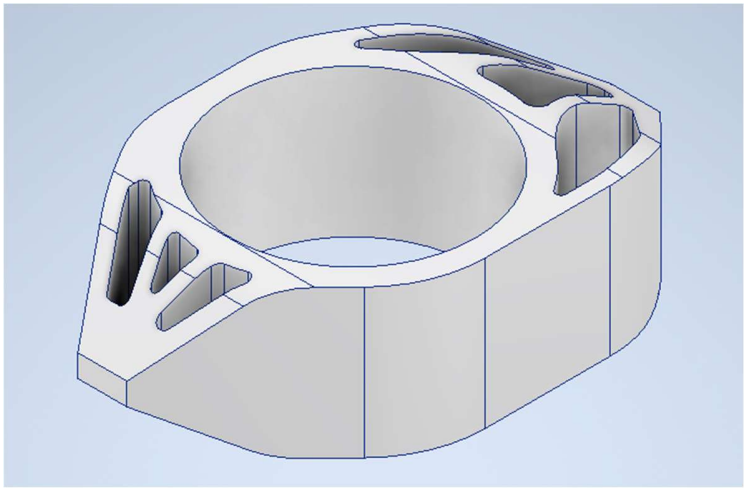

Figure 3.1.1 illustrates one of the first concept design used to gain an idea of the possibilities and limitations.

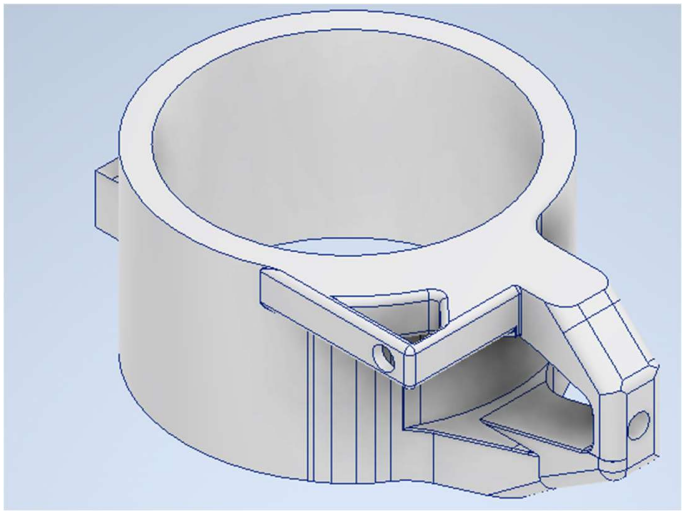

Figure 3.1.2 illustrates one of the first concept design used to gain an idea of the possibilities and limitations.

These designs were primarily created to explore possibilities, as important design parameters were still missing at the time of their creation. These parameters mainly included the necessary direction of the brackets and the internal dimensions of the centre hub. However, they could still be used to decide to proceed with a design similar to the one depicted in Figure 3.1.2, rather than the one in Figure 3.1.1, which closely resembles previous designs used at ION Racing. This decision was influenced by the increased diameter and thickness of the centre hub in the former design, making it heavier than the latter, which utilizes less material. When more information about the brackets requirements for the upright was gained by the other ION Racing members updated designs were made. This can be observed in Figure 3.1.3.

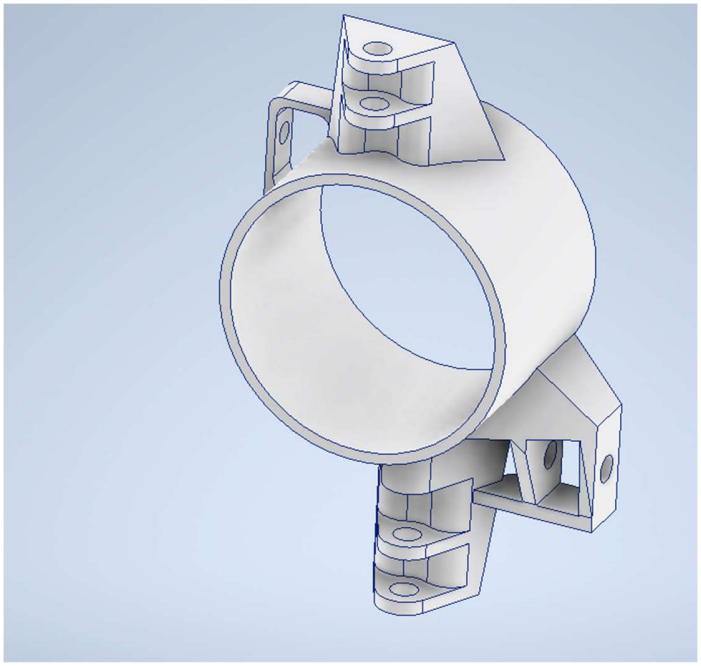

Figure 3.1.3 illustrates the upright in the concept level design phase.

After this the first concept requirements from other ION Racing members for the inner dimensions of the upright was given. In Figure 3.1.4. the required material for the centre hub can be observed. The more complex design then previously is due to that it now will be a gearing inside the upright. This needs more space than before and a bigger diameter in the centre.

Figure 3.1.4 illustrates the hub requirements form the concept phase. This is the required material dimensions. The reason for the bigger diameter inside is to accommodate for the gearing which will be inside the upright.

With this information the final concept designs could be made. This can be observed in Figure 3.1.5. At this stage, which manufacturing method to base the design around was considered. To do a basic evaluation of the possibilities.

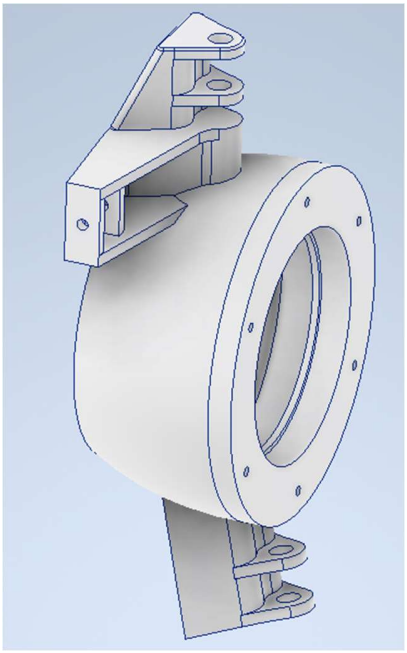

Figure 3.1.5 illustrates final concept design. This includes points for the brackets and the correct direction in addition to the design of the centre to accommodate for the gears and the bearings.

3.2 Manufacturing method

To quickly test the viability of different manufacturing methods, a shape generator simulation was performed on the final concept design, as illustrated in Figure 3.2.1. The result from this simulation showed that it would be possible to reduce the weight by 9% using additive manufacturing over traditional methods. This does not account for the weight loss from employing a hollow core similar to NTNU Revolve, which would lead to even greater weight reduction. However, after evaluating the cost of additive manufacturing, both the more complex design process and manufacturing, it was decided that this weight reduction would not be worth the constraints for ION Racing at this stage. Nevertheless, it was deemed a valuable consideration and likely a direction for future refinement of this design within ION Racing. For this reason, this concept was abandoned in favour of further development of the more traditional conceptual design.

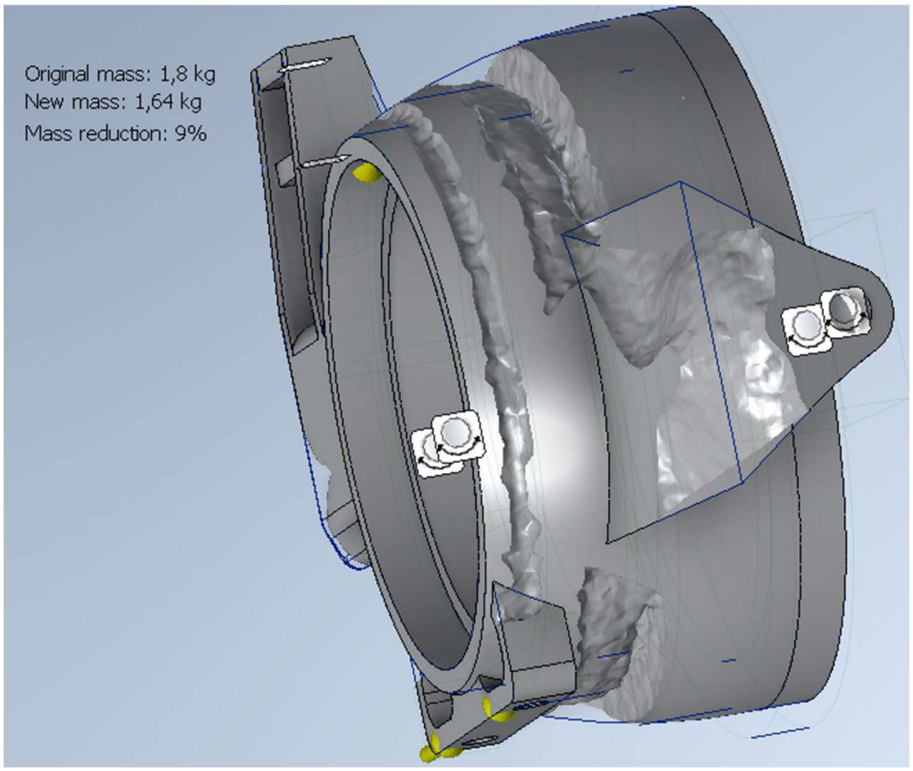

Figure 3.2.1 illustrates the possible gains form additive manufacturing. The blue line represents where the original design was, and one can observe where material has been removed by the uneven surface. In the top left corner different results from the simulation can be read. This includes the Original and new mass, and what percentage of weight reduction this equates to.

3.3 Stress simulation method

CAD modelling and simulation allows for faster identification of maximum stress, especially in complex figures that would be otherwise difficult to analyse. However, one must verify that the simulation is correct. This ensures that any errors made by the student during the simulation process are excluded, and also minimizes the likelihood of software errors.

During the experiment, the average mesh size was set to 0.01 which contrasts with the standard 0.1. This significantly affected both where the biggest stresses and their size were simulated. To make the analysis as correct as possible a convergence curve was also made for the upright developed in this project. The results from this can be observed in Figure 3.3.1. The graph illustrates that the selected average element size in the mesh of 0.01 is a good compromise because after this the simulation only takes longer with little gain in accuracy.

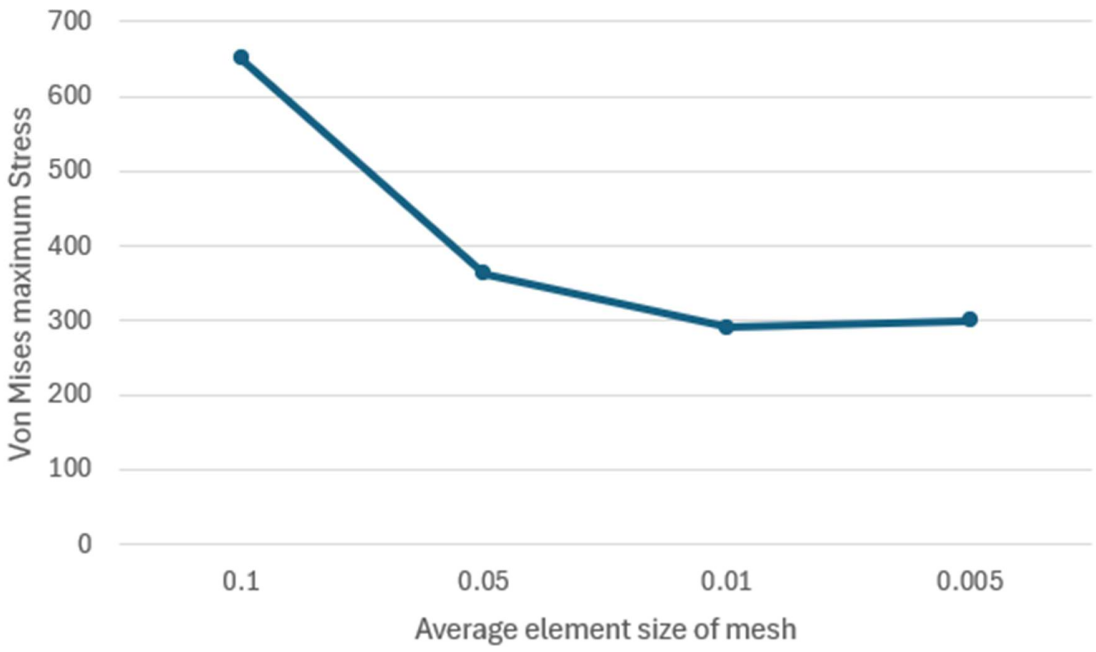

Figure 3.3.1 illustrates the convergence curve for the simulation of the stresses in the Upright with the change in mesh size. The plot was made by changing the average element size of the mesh on the upright and simulating the stresses, Then the results were plotted.

This analysis involves calculating the bending stress, as it represents the most significant stress on the component. Ensuring that the bending stress is lower than that observed in the simulated scenario, which also includes multiple smaller stresses, is crucial. The formula used to calculate bending stress is:

$$\sigma_{bending} = \frac{M * v}{I}$$

Where “M” is the moment and “v” is the distance from the edge to the neutral axis of the beam. When a beam is subjected to bending, it experiences tension on the top side and compression on the bottom side. This creates a distribution of stresses throughout the depth of the beam. The bending stress increases linearly from zero at the neutral axis, which is at the centre of the beam to a maximum value at the outermost of the beam.

The reason that the maximum bending stress occurs at the edges of the beam is because this is farthest away from the neutral axis, resulting in a larger moment arm. The last variable is the moment of inertia, symbolised with “I”. The formula for the moment of inertia for a square is given by (Vedantu, 2024).

$$I = \frac{a^4}{12}$$

Where “a” is the length of the two sides of the beam, this length can be seen in Figure 3.3.2.

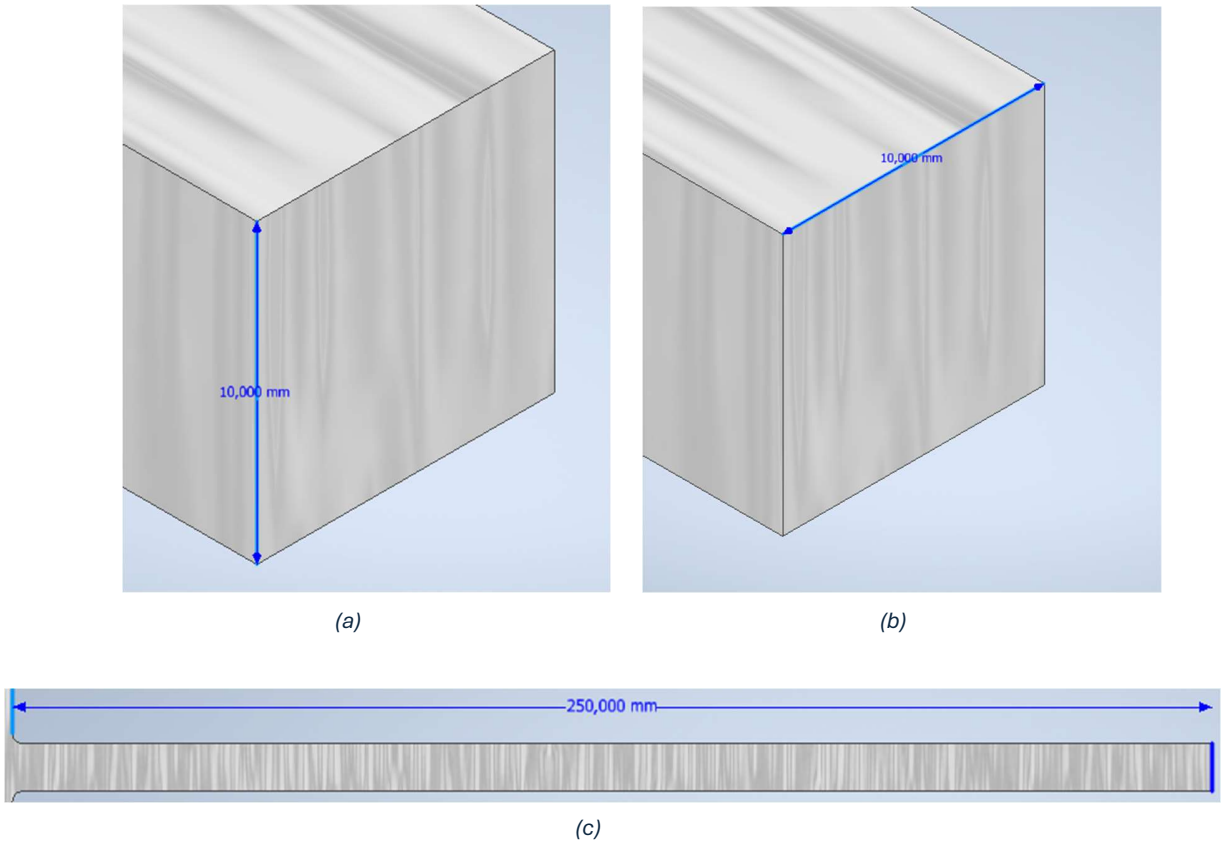

(a) *(b)*

(c)

Figure 3.3.2 (a) and (b) shows that the test beam has a 10x10 mm cross-section. Part © illustrates that the beam has a length of 250 mm.

Therefore, the moment of inertia “I” can be calculated.

$$I = \frac{0.01^4}{12} = 8.33 * 10^{-10}$$

And the “v” the distance from the neutral axis is.

$$v = \frac{a}{2} = \frac{0.01}{2} = 0.005$$

With the force F being 1000 Newton being spread over the top surface, the bending moment and “x” is therefore the length of the beam divided by two. Due to the force acting evenly and the length of the beam being 0.25 meters which is illustrated in Figure 2.3.2 (c) one can perform the calculation the following way.

$$M = F * x = 1000 * \frac{0.25}{2} = 125\ Nm$$

Plotting this in the formula for bending stress.

$$\sigma_{bending} = \frac{125\ Nm * 0.005}{8.33 * 10^{-10}}$$

$$\sigma_{bending} = 750\ MPa$$

To control the simulation method this calculated stress of 750 MPa must be compared with a similar simulation. A simulation was therefore preformed in Autodesk Inventor. With the same shape and dimensions. The only difference is that for the simulation it was decided to mount the beam to a horizontal beam, because this better represents an upright. In addition to this the stress was simulated in all directions using Von Misis stress, in contrast to the bending stress which was only calculated for one direction. This was assumed acceptable because the bending stress in the direction along the beam was anticipated to be the biggest stress.

When preforming the simulation fixed constraints were set at the ends of the vertical beam, illustrated in Figure 3.3.3 (a) with the white icons. Further the force of 1000 N was applied over the top surface of the horizontal beam, illustrated by the yellow arrow. Preforming the simulation gave the results observable in Figure 3.3.3.

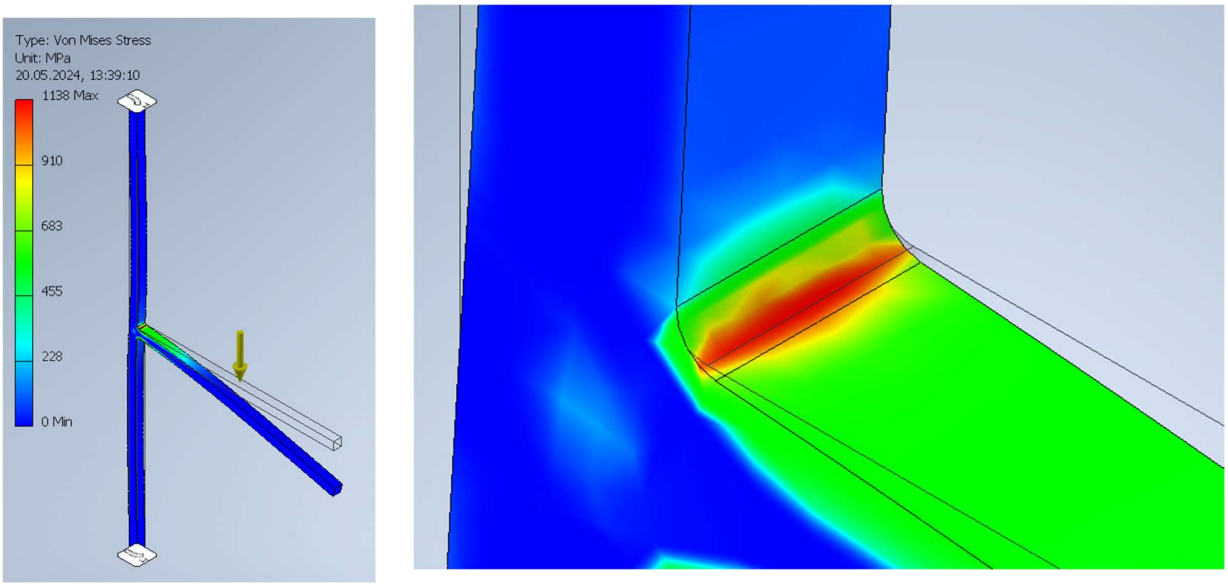

(a) *(b)*

Figure 3.3.3 illustrates the results obtained from the simulation test conducted in Autodesk Inventor. This simulation was performed to ensure the reliability of the results. In part (a), the color-coded stress bar on the left indicates the magnitude of stress at various points, this shows a maximum stress of 1138 MPa. Part (b) provides a detailed view of the area experiencing the highest stress, located at the edge of the beam within the fillet between the two edges. The fillet has a radius of 1 mm, chosen as the optimal and simplest representation.

This simulation gives a maximum stress of 1138 MPa, revealing a discrepancy between the calculated value and the simulated value larger than anticipated. This magnitude of error is unacceptable for achieving a lightweight design, as it necessitates over-dimensioning and results in a heavier structure than required. The error is suspected to originate from the vertical beam's deflection observed in Figure 3.3.3 (a), which did not constrain the horizontal beam as assumed in the calculations. This misrepresentation likely caused the higher stress observed in the simulation.

To address this issue, a second simulation was conducted, removing the vertical beam, and directly constraining the horizontal beam. The initial approach was selected because it better represents the upright compared to considering only the horizontal beam. However, adjustments in the second simulation were necessary to correct the initial misassumptions and provide a more accurate representation of the stress. It was also decided to analyse the stresses in the longitudinal direction due to this representing what is calculated better. This is because the calculated bending stress is only one direction and the simulated Von Mises stress is in all directions. This difference was therefore removed. This like the change in simulated design, makes the test represent the analysis used in the design prosses worse. However, after discussion with the supervisor it was determined better to make the test more accurate than make it match the used simulation. This new simulation can be observed in Figure 3.3.4 and resulted in a result slightly closer to the calculated result.

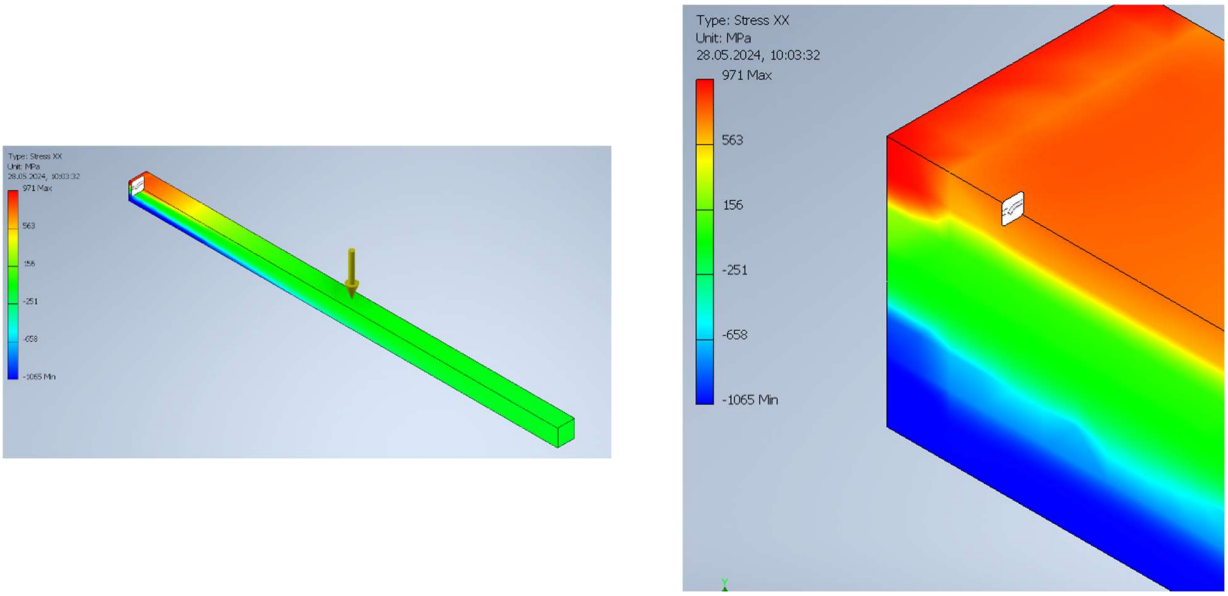

(a) *(b)*

Figure 3.3.4 illustrates the second simulation. In Figure (a) the arrow illustrates where the force of 1000 Newton acts and the white symbol represents the fixed constraint. On the left of the figure a bar illustrates what magnitude of stress the different colours on the beam symbolise. The same is the case for Figure (b) however it is a zoomed-in picture on the fixed edge where the stresses also are the highest.

With the result from the second simulation being 971 MPa, it matches the calculated maximum stress of 750 MPa significantly better. However, the calculated stresses are still smaller than the simulated ones. Some of this is anticipated to be due to that stress concentration is included in the analytical method used in the simulation. This is not included in the simple bending stress calculation. These stress concentrations are at the edge of the beam. Therefore, one can eliminate this by calculating the stress at a small distance from the edge and comparing this to the simulation instead.

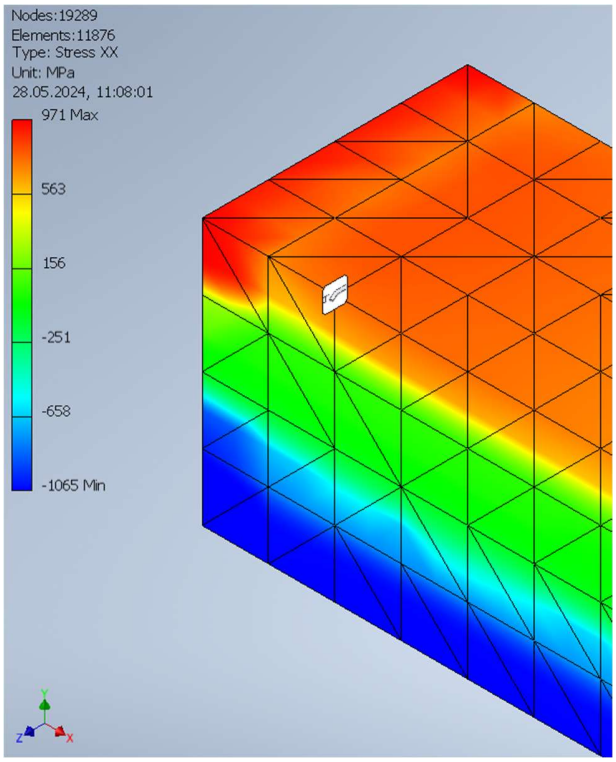

Figure 3.3.5 illustrates the second control analyses. In the bar in the left of the figure one can observe what magnitude of stress the different colours on the part symbolise. The lines over the part is the mesh. This divides the part into smaller elements, which makes it possible to for the simulation tool to find the stress distribution.

It was decided to perform this calculation 4 elements away from the edge. As shown in Figure 3.3.5, there are 4 elements. This corresponds to a length of 10 mm, so each element's side is 2.5 mm, and the stress 10 mm from the edge is calculated. Performing the same calculation as previously, this gives:

$$M = F * x = 1000 * 0{,}124 = 124\ Nm$$

$$\sigma_{bending} = \frac{124\ Nm * 0.005}{8.33 * 10^{-10}}$$

$$\sigma_{bending} = 744\ MPa$$

This is only a small decrease in calculated stress, however if one looks at the simulation there is a significant colour change. From observation the colour looks to represent the middle of 971 and 563 MPa. One could argue that this is too much compromise to reach the wanted result. And this is a fair argument. However, due to previously mentioned arguments for why the other methods were wrong it is believed that this still proves that using Inventor simulation gives an accurate result.

4. System-level design

With the limitations set by the selected concept and the rest of the wheel assembly, the focus in the system-level design phase is to further develop the chosen design and control that it will withstand the conditions it will experience.

4.1 General design

In the system-level design, multiple decisions must be made, starting with determining how to achieve the required camber angle. In Figure 4.1.1 one can observe two possibilities. Figure (a) is the previous design used by ION racing.

This consists of three parts. This is mainly because the camber angle and the angle of the rods connecting to the car were not set before the design was made and with this design this could be changed afterwards. This was a quite flexible design; however, it was also heavier than required. Instead, one can use a lighter and less flexible design illustrated in Figure 4.1.1 (b). In the development of this upright, the camber angle is already set as well as the angle of the tie rods. For this reason, the design in Figure 4.1.1 (b) was selected.

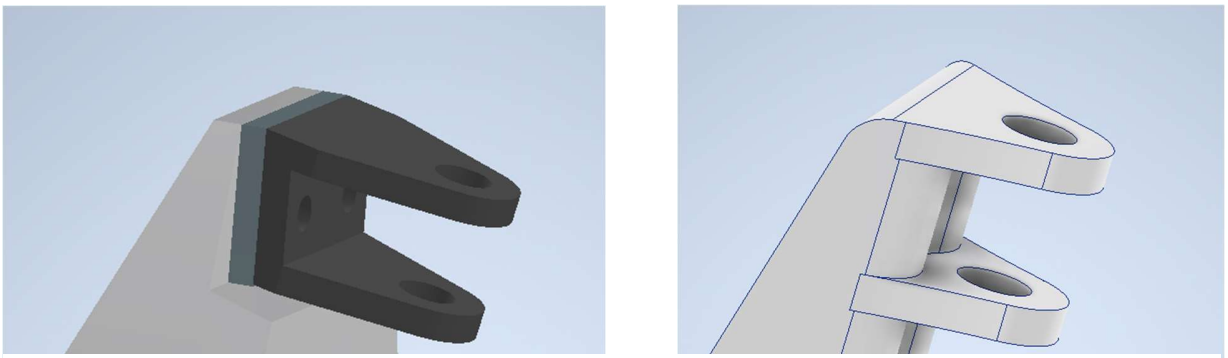

Figure 4.1.1 illustrates two ways to achieve a camber angle. Figure (a) consists of three parts and Figure (b) consists of just one.

(a) *(b)*

Secondly how to remove unnecessary material must be decided. In Figure 4.1.3 one can observe that this usually is done by removing triangles. This is because this is a shape that spreads the forces and thus minimises the stresses which is illustrated in Figure 4.1.2. For this reason, this was also used in the design of this up-right.

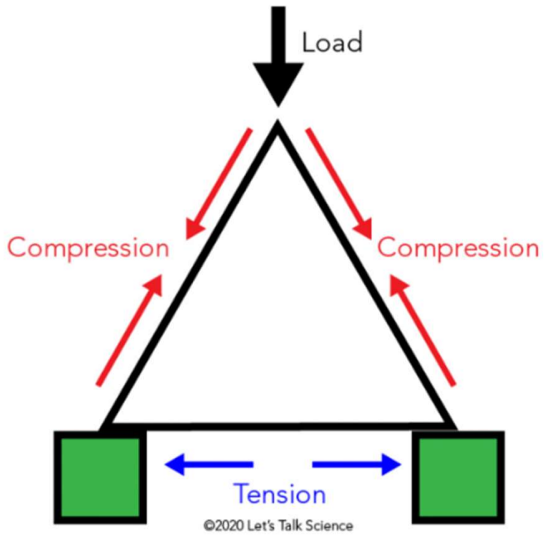

Figure 4.1.2 Illustrates how a triangle distributes a force evenly (letstalkscience, 2024).

In addition, the backside can be hollowed out as illustrated in Figure 4.1.3(b) and (d). This approach was also applied in the design of this upright, maintaining more material in pillars on the sides as shown in Figure 4.1.3(d). The reason for not dividing it into triangles is that doing so is not so straightforward for this part, with no obvious solution.

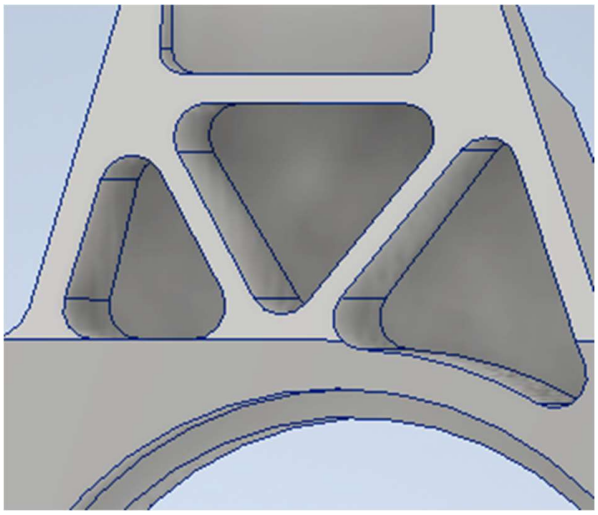

(a)

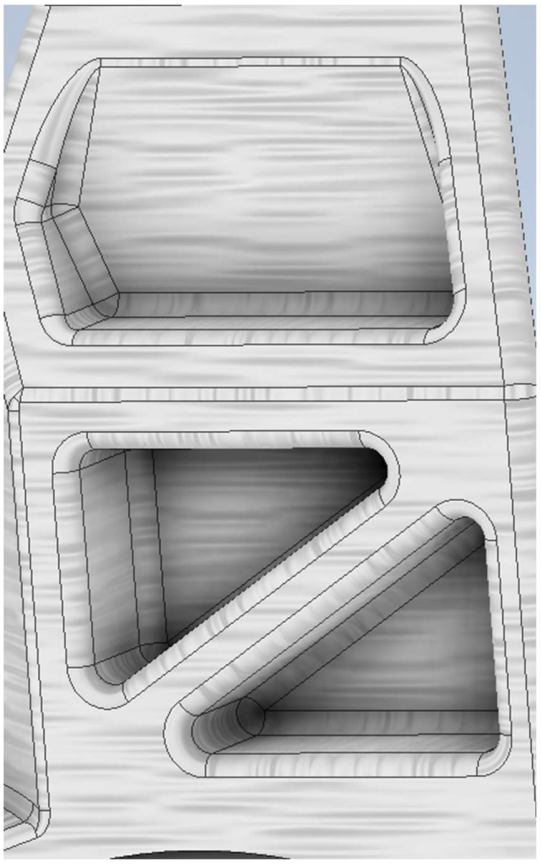

(b)

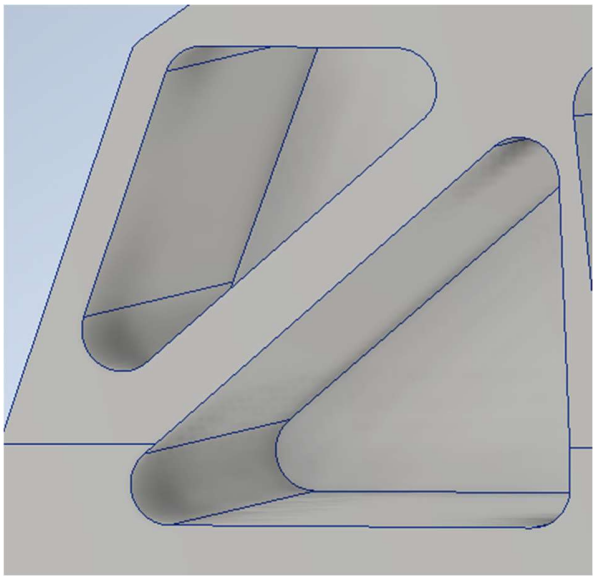

(c)

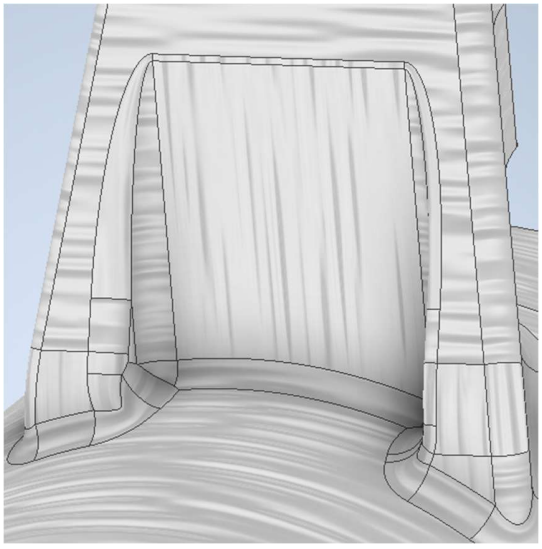

(d)

Figure 4.1.3. illustrates different methods to remove material where it is unnecessary. Figure (a), (b) and (c) illustrate that this was achieved by removing triangles. This is a shape that distributes the force good and thus the stresses. Figure (b) and (d) illustrate a shallower square removed.

Triangles were also used in the bracket for the tie-rod on the side of the upright. Several design possibilities were considered, which can be observed in Figure 4.1.4.

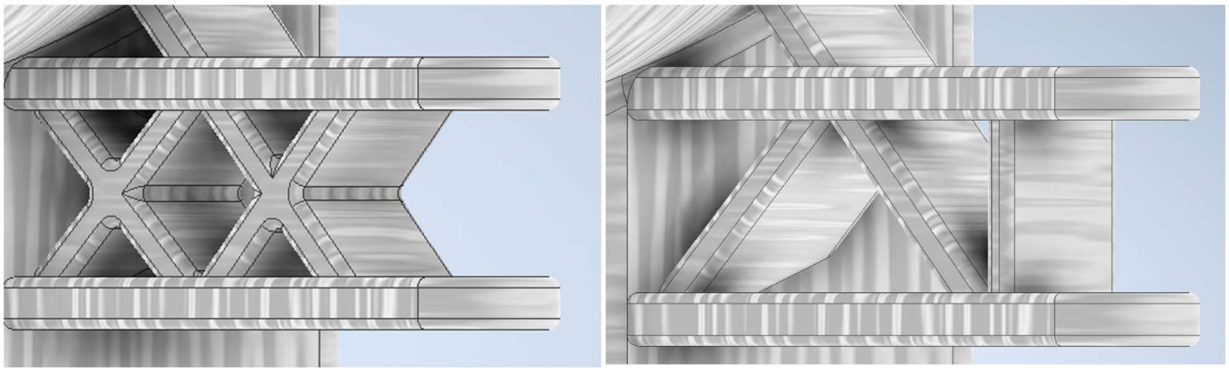

(a) (b)

Figure 4.1.4 illustrates distinctive design opportunities considered in the concept design phase. Figure (a) is a stronger but possibly unnecessary strong and heavy design and Figure (b) illustrates a lighter design.

The main difference between the two designs is that the design in Figure (a) is divided into more smaller triangles. This makes it stronger, however this at the cost of increased weight. Because the design in Figure (b) is lighter, and it does not need to be stronger this design was chosen. This follows the project's design philosophy of making a light design. The philosophy is also followed when selecting design (a) in Figure 4.1.4 over design (b). Both are also made of triangles.

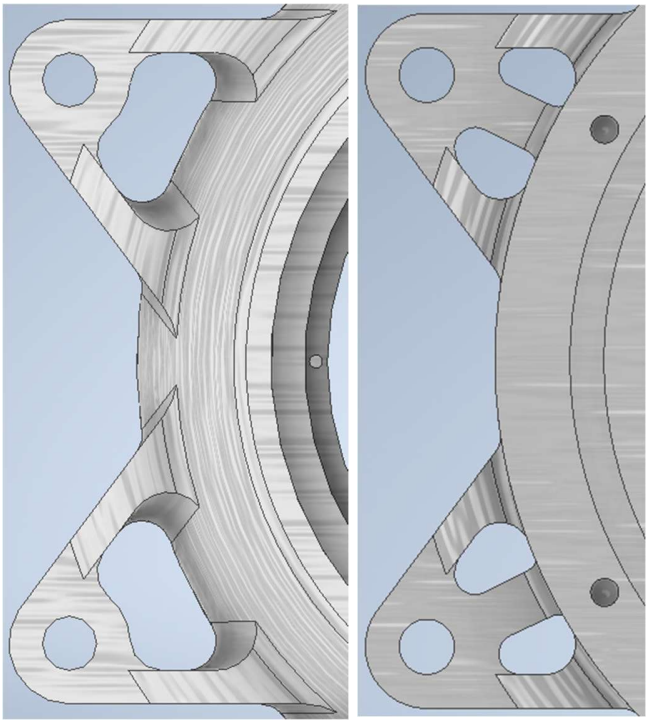

(a) (b)

Figure 4.1.5 illustrates two distinctive design possibilities for the brake bracket for the front upright. The design in Figure (a) is a straightforward design with angled support which is needed for the upwards braking force acting. Figure (b) is based on the same design however it also has support in between the two main supports, which specially makes it stronger against a horizontal force.

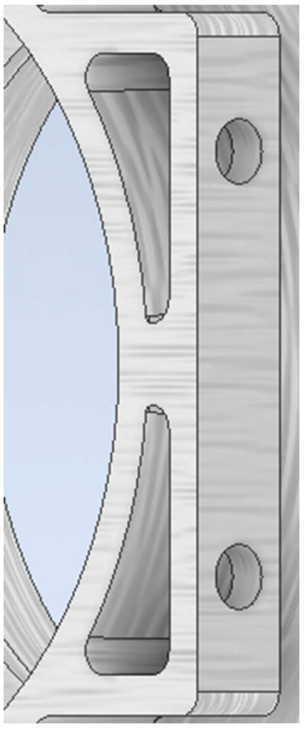

Figure 4.1.6 illustrates the brake bracket for the back wheels, where there is no distinctive design decision.

Design (a) is designed with angled support to withstand the breaking force which acts upwards. Design b in Figure 4.1.5 is based on design a however with an extra support added in between to make it stronger. This was however determined to mainly work against horizontal forces. In this case, this was not necessary because the main force is the break force, which acts laterally upwards. Therefore, design (a) is used, due to it being lighter. Figure 4.1.6 illustrates the different design for the brake bracket for the back wheel. It needs to be different due to different brakes. Due to the design of the brakes, there are only minor changes that can be made, and the design is nothing special.

4.2 Stress analysis

To ensure the part is optimally designed, avoiding both over-engineering, which results in excessive weight, and under-engineering, which compromises structural integrity, a series of stress analyses and calculations were performed.

This is important for an engineer to make sure the design will be able to handle the expected conditions it will be exposed to. This includes fatigue, corrosion, impact forces and constant forces.

In the case of a Formula student car corrosion and fatigue is mostly overlooked. This is because the cars and all their parts only are required to last one season. In ION racings case this only includes a maximum of 5 hours of testing before the race in Silverstone. And about the same time during the race. In this short lifetime, neither corrosion nor fatigue is going to be the limiting factor.

The upright should not be exposed to impact; however, this can be hard to guarantee since ION Racing consists of students, and mistakes can happen in the handling of the parts. If one decides to build the parts out of composite materials, one must therefore consider that this material is fragile when exposed to impact and hard to repair if it breaks. Aluminium, however, is much more resistant to impact; therefore, this issue does not require as much focus.

For the above-mentioned reasons, the stress analysis was based on the maximum forces experienced during racing. Figure 4.2 below shows a result after doing a simulation in Autodesk Inventor. The accuracy of these were improved during the design process therefore the final method is discussed in the detail design stage.

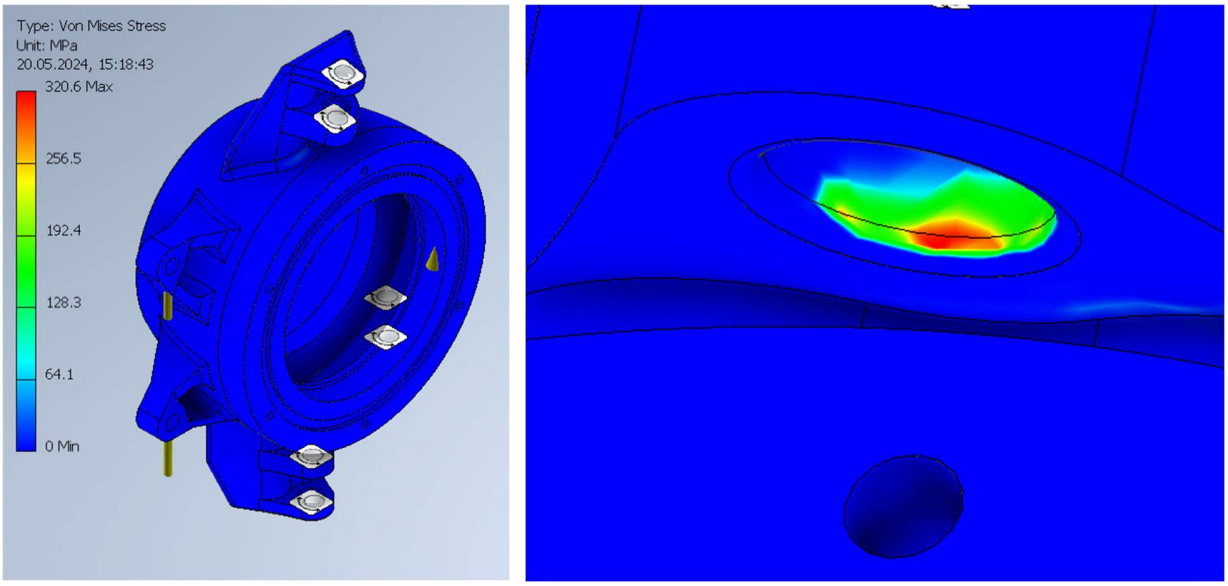

(a) *(b)*

Figure 4.2 illustrates an example of a stress analyses of an upright in the detail design phase. On the left, in Figure (a) one can observe the scale of the different colures. This shows that the maximum stress is 320 MPa and where this is shown in red. In part (b) one can see a zoomed in picture of where this is.

4.3 Force calculation

Table 4.3 illustrate calculation results of forces acting on the upright given in Newtons, performed by other ION members. The forces are divided into vertical, lateral, and longitudinal. Where lateral is perpendicular to the driving direction and longitudinal is parallel to the driving direction.

Vertical Z	Front		Rear		Max	Min
	Outer	Inner	Outer	Inner	1858.54	25.74
Static	942.41		941.87		Max Front	Min Front
Acceleration	404.32		1316.19		1858.54	404.32
Braking	1858.54		25.74		Max Rear	Min Rear
Cornering	1884.81	0.00	1883.74	0.00	1883.74	25.74

Lateral Y	Front		Rear		Max	Min
	Outer	Inner	Outer	Inner	4276.08	0.00
Static	0.00		0.00		Max Front	Min Front
Acceleration	0.00		0.00		4278.53	0.00
Braking	0.00		0.00		Max Rear	Min Rear
Cornering	4278.53	0.00	4276.08	0.00	4276.08	0.00

Longitudinal X	Front		Rear		Max	Min
	Outer	Inner	Outer	Inner	4980.89	68.97
Static	0.00		0.00		Max Front	Min Front
Acceleration	1083.57		1566.92		4980.89	0.00
Braking	4980.89		68.97		Max Rear	Min Rear
Cornering	0.00	0.00	0.00	0.00	1566.92	68.97

Other members of ION Racing did the biggest part of the force calculations for the car. The results from this are shown in Table 4.3. These Calculations show that the worst-case scenario in the front is when the car is braking maximum while turning maximum, and for the rear it is when accelerating and turning. The reason for this is the transfer of weight when accelerating and decelerating. Figure 4.3.1 visualises this and makes it easier to understand. The reason the weight transfer affects the breaking and acceleration force at the front and rear wheels is due to friction.

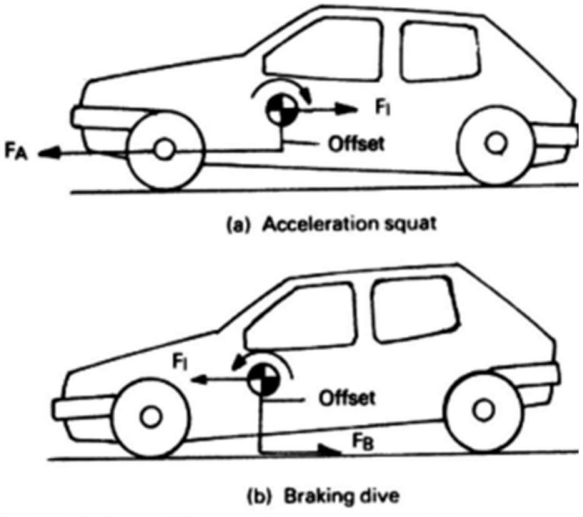

Figure 4.3.1 Visualizes the squat and dive of a car when braking and accelerating. Part a symbolizes how the centre of gravity of a car moves when the car accelerates and part b when deaccelerated (Bhosale, 2024).

The formula for the friction of the tyres is.

$$F_{friction} = \mu * N$$

Where μ is the coefficient of friction, which is assumed to be constant at 2.6, N is the normal force that changes when the centre of gravity shifts. This shift is the reason why the forces at the front and rear differ. When the car brakes, the centre of gravity moves forward. Consequently, the normal force at the front increases, which in turn increases the friction force, resulting in a greater braking force. Conversely, at the rear, the opposite occurs (Bhosale, 2024).

However, one cannot put all forces directly into a simulation. The force experienced when turning must be converted. In Figure 4.3.2 one can see that there is only an outer force. This is due to incorrect measurements on the current car which is what the numbers are based on. However, it is imperative to ensure that the force exerted on the inner component does not exceed that on the outer component. Consequently, both the inner and outer forces are equated to the same value. This precautionary measure represents the worst-case scenario for the inner component, thereby mitigating any potential risks associated with unequal force distribution. These are given as vertical and lateral forces. Thus, it must be converted

to one force to perform a simulation. Applying the methodology employed in race car design, the following approach can be adopted for the front upright: (Seward, 2022).

$$F_{outh} = \frac{(W_{lateral} * R_r) - (W_{vertical}(l_1 + l_2)}{l_1} \text{ (Seward, 2022)}$$

Where all the different variables are given in Figure 4.1 (a) below.

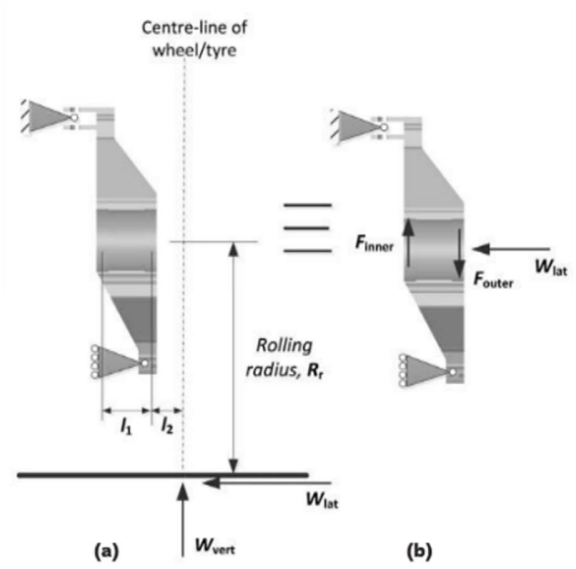

Figure 4.3.2 visualizes what the variables and forces of an upright used in the calculations are (Seward, 2022).

This gives the values of the variables:

$W_{lateral}$ = 4279 N

$W_{vertical}$ = 1885 N

R_r = 0.26 m

l_1 = 0.0605 m

l_2 = 0.049 m

Plotting this into the formula one gets.

$$F_{outher} = \frac{(4279 * 0.26) - (1885 * (0.0605 + 0.049)}{0.0605}$$

$$F_{outher} = 17\ 943\ N$$

The inner force can be calculated using the following formula, also from race car design (Seward, 2022).

$$F_{inner} = F_{outer} + W_{vertical}$$

$$F_{inner} = 17\,943\ N + 1\,885\ N$$

$$F_{inner} = 19\,828\ N$$

These are the forces used in the simulation shown in figure 4.4.1. However, as mentioned previously, on the rear upright the acceleration force is bigger than the brake force. Therefore, different values must be used. Firstly, what the different parameters symbolise is given in Figure 4.3.3.

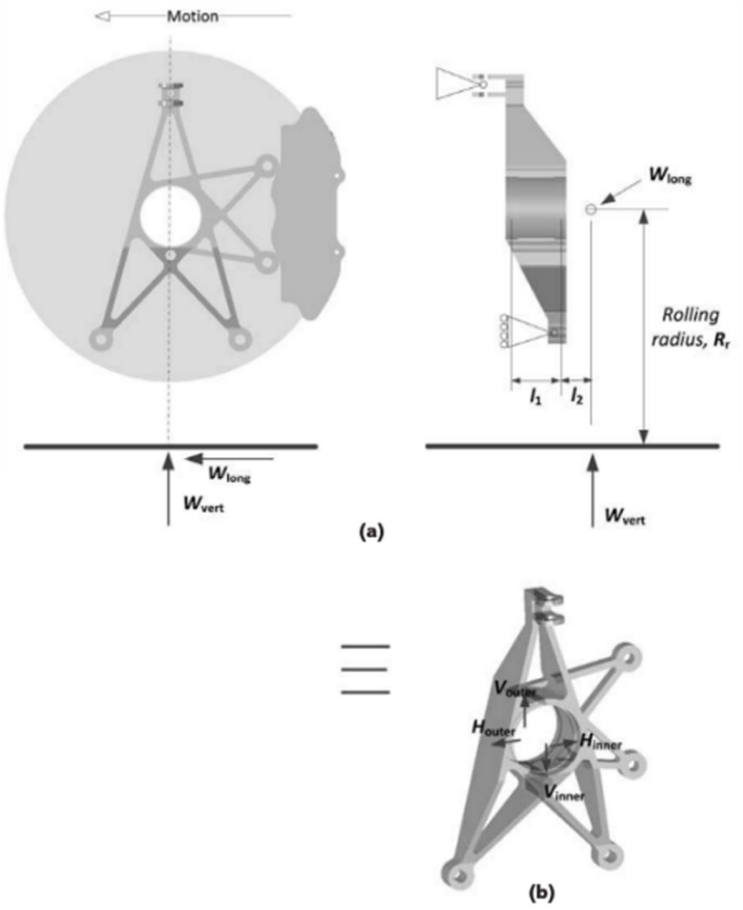

Figure 4.3.3 illustrates what different parameters symbolise in the calculation of forces acting on the rear upright (Seward, 2022).

Too convert the forces so that they can be used in simulation is done using the method of Race car design (Seward, 2022).

$$V_{outer} = \frac{W_{vertical} * (l_1 + l_2)}{l_1}$$

$$H_{outer} = \frac{W_{longitudional} * (l_1 + l_2)}{l_1}$$

Summing the vertical forces.

$$V_{inner} = V_{outer} - W_{vertical}$$

Summing horizontal forces.

$$H_{inner} = H_{outer} - W_{longitudional}$$

With the given and previously calculated values being.

$W_{longitudional}$ = 1567 N

$W_{vertical}$ = 1317 N

l_1 = 0.0605 m

l_2 = 0.049 m

Plotting this into the formulas one gets.

$$V_{outer} = \frac{1317 * (0.0605 + 0.049)}{0.0605}$$

$$V_{outer} = 2384\ N$$

$$H_{outer} = \frac{1567 * (0.0605 + 0.049)}{0.0605}$$

$$H_{outer} = 2837\ N$$

$$V_{inner} = 2384 - 1317$$

$$V_{inner} = 1067\ N$$

$$H_{inner} = 2837 - 1567$$

$$H_{inner} = 1270\ N$$

These results will be used when simulating the back upright.

4.4 Simulation

Due to the lack of knowledge about the finite element method a simpler simulation is done in Autodesk Inventor instead. After thoroughly controlling the accuracy of this method in the concept design phase, this is determined as the best results one can gather, and good enough for this case.

Using the calculated external forces the stresses in the upright were simulated. Figure 4.3.1 below. This shows that the stresses experienced in the part are far less than the yield strength of the material.

To clarify yield strength is a critical mechanical property of materials, particularly metals and alloys. It refers to the maximum amount of stress that a material can withstand without undergoing permanent deformation or failure. However, when a material is subjected to stress below its yield strength, it will deform elastically, meaning it will return to its original shape once the stress is removed (Engineers edge, 2024) (Edurev, 2024).

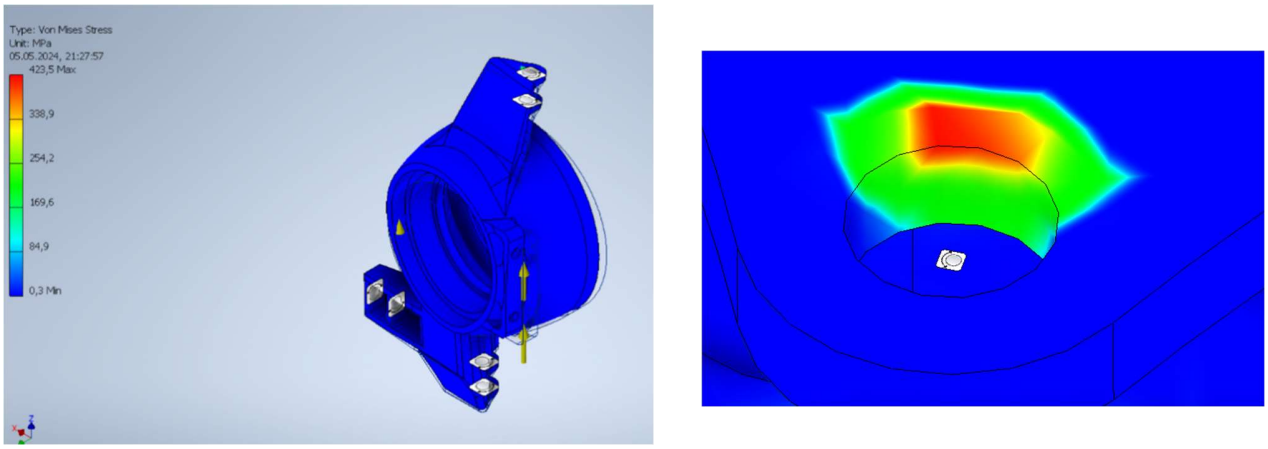

(a) *(b)*

Figure 4.4.1 Illustrates Von Mises stress simulation of the front left upright performed in the concept level design phase. On the left, in Figure (a) one can see what stress the different colours represent. And in Figure (b) one can see a zoomed-in picture of where the biggest stress is. This is in the bottom bracket.

Due to the stresses being significantly lower than the yield strength of the material, there was potential to remove unnecessary material and thus reduce weight. To identify removable material, the "shape generator" function could be employed. However, further analysis of the simulation report revealed a potential issue with the placement of the force from the outer bearing during turning. The method can be observed in Figure 4.3.2 (b). This issue arose because the force was applied to a circular surface. Figure 4.4.2 (a) highlights this concern through the colour variation around the hub. In Figure 4.4.2 (b), the force application during simulation is illustrated, with the arrow indicating force on one side of the circular plane. This, coupled with the simulation results suggesting the force acted only on one side, raised suspicions. Consequently, the simulation method was reviewed and controlled.

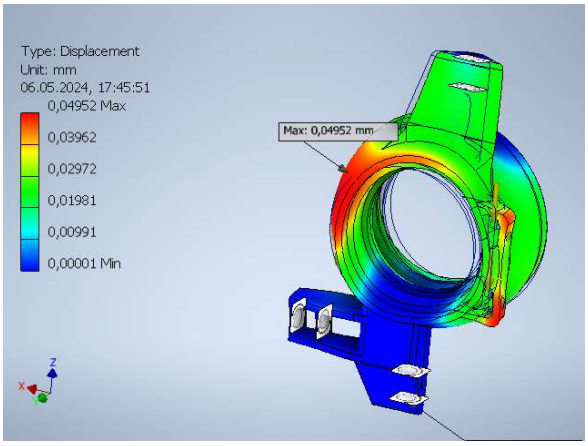

(a)

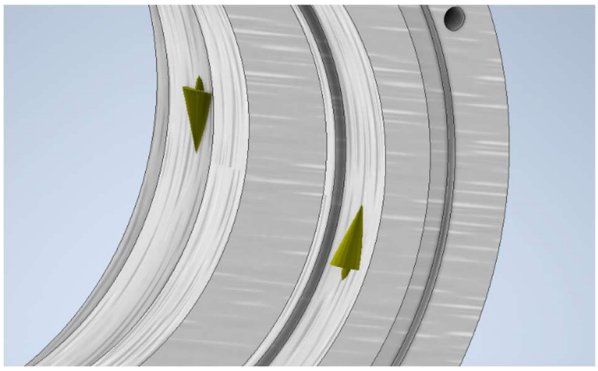

(b)

Figure 4.4.2 (a) illustrates the deformation of the upright from simulation in system-level design process. There one can observe that the deformation is not even around the hub. This can be observed by the difference in colour. In the bar to the left how big the deformation is can be observed. In Figure (b) one can observe how the force arrows are illustrates when performing a simulation.

One way of checking whether this simulation method is faulty is to do a simple simulation where one could detect if this was the case. For this reason, the simulation in Figure 4.4.3 was performed.

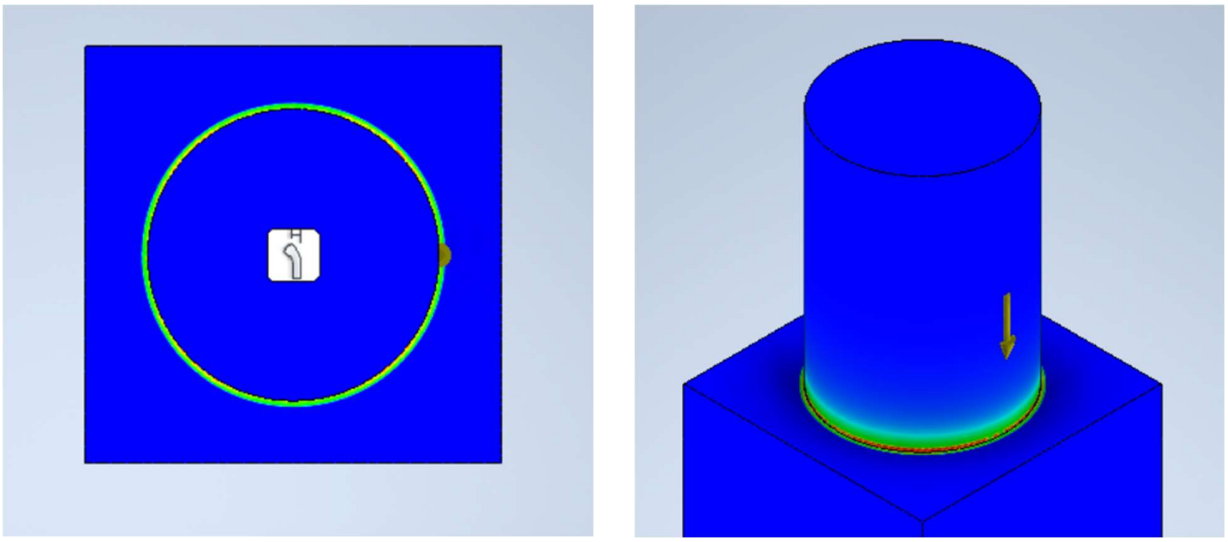

(a) (b)

Figure 4.4.3 Simple test of simulation method to control whether the force is spread evenly over a circular surface area. The arrow symbolises where the force is applied, however as the simulation result illustrates this indication is misleading. The force is evenly spread over the circular surface by the evenly coloured circle illustrated in Figure (a).

This shows that the simulation method indeed is correct and that the force is evenly distributed. The reason for the uneven distribution is therefore not due to a simulation error and most likely due to that the upright is not symmetric.

Because the stresses were so much smaller than the yield strength of the material the possibility of removing unnecessary material and thus making it lighter was investigated. His was done using the function “shape generator” in Autodesk Inventor.

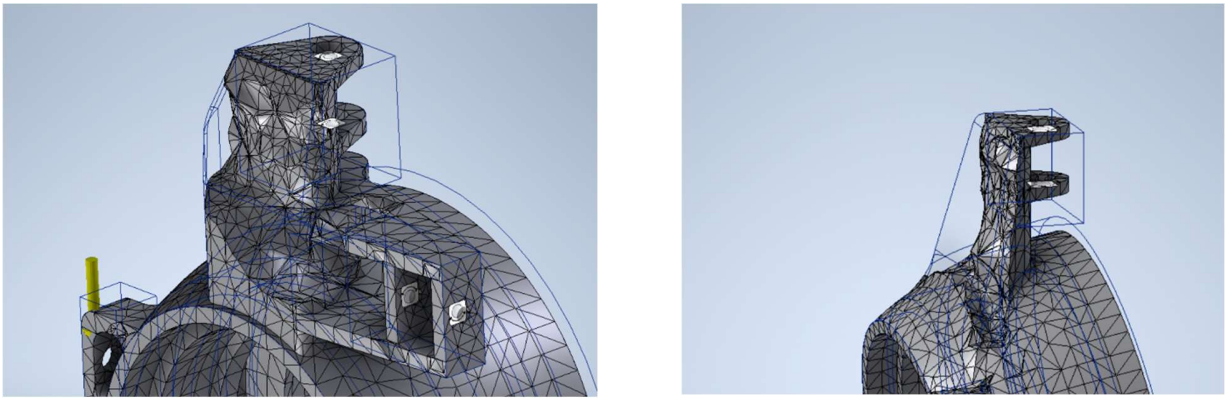

(a) (b)

Figure 4.4.4 illustrates the material possible to remove from the up-right in the concept design phase using shape generator. This removes where the stress is the lowest with the goal of removing a percentage of mass. In this simulation this was set to 8%.

Using this information the brackets were modified using methods previously discussed in the in chapter 4.1.

5. Detailed design

Taking the results from the performed simulations, and updated information from co-projects at ION were considered doing the final adjustments of the design. With an updated design with both changed inner dimensions, due to changed gearing. In addition, some weight was removed. Then a simulation was performed with pin support in all connections to the frame and more correct forces below. With the breaking force being spread over the two holes in the brake bracket.

$$F_{breaking} = 4981\ N$$

$$F_{outh} = 17\ 943\ N$$

$$F_{inner} = 19\ 828\ N$$

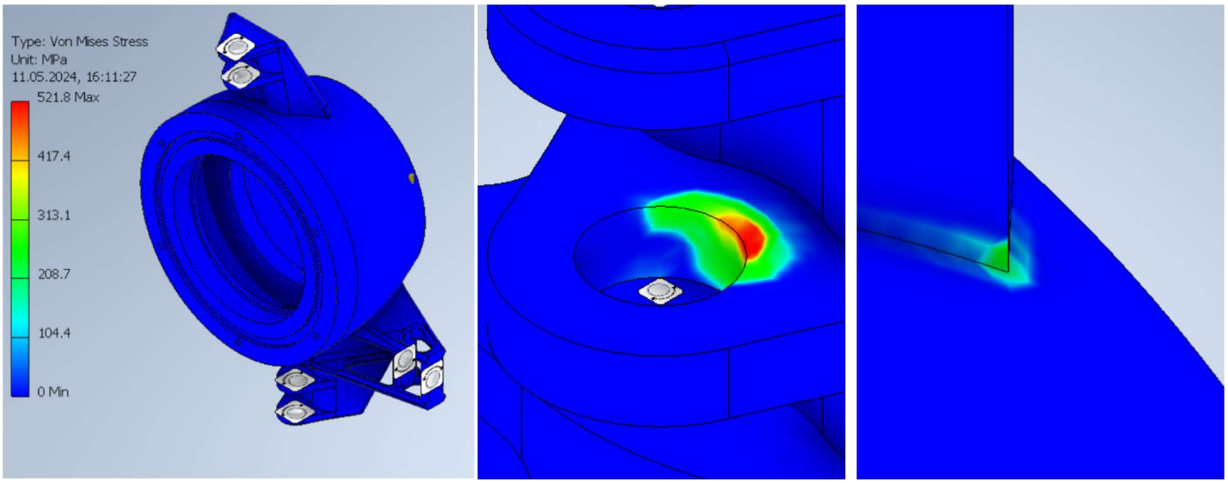

(a) (b) (c)

Figure 5.1 illustrates results from a more accurate simulation of the updated design in the detail design phase. In Figure (a) one can see the complete up-right with a stress to colour scale to the left. In Figure (b) and (c) one can observe zoomed-in on parts where the biggest stresses are.

The braking force was now set to be acting upwards when the brake bracket is mounted on the rear end of the front upright, this is different on the rear upright where the biggest force is the acceleration. And the bearing forces were set to be acting down on the outer and upward on the inner, which is shown in Figure 5.1.

The results are shown in Figure 5.1. This shows that the maximum stress is 522 MPa. This is more than the yield strength of 503 MPa for Al 7075 and therefore too much. However, this is at the point where the upright is bolted to the frame. This can be seen in Figure 5.1 (b). To solve this the thickness of the bracket was changed from 5 to 7 mm, with hopes this would decrease the stresses. The other places where the stresses are the biggest are in the sharp corners which is shown in Figure 5.1 (c). This can be made better by smoothing out the corner with a fillet. In Figure 5.2 the effects of these changes can be seen.

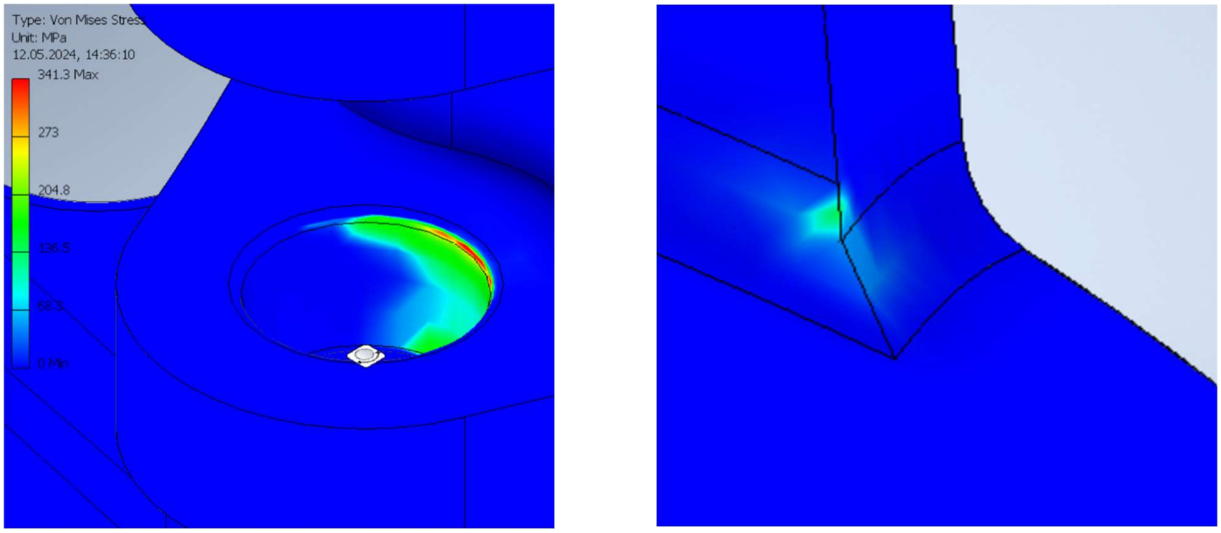

(a) *(b)*

Figure 5.2 illustrates results from a more accurate simulation of the updated design in the detail design phase. In Figure (a) the stress to colour stress on the left as well as where the biggest stress is. In the connection to the frame of the car. Figure 5.2 (b) illustrates the effect of a fillet compared to Figure 5.1 (c).

The new simulation reveals that the maximum stresses now experienced are below the yield strength of the selected material, Al 7075, with a safety factor of 1.47, indicating an acceptable level of structural integrity. Consequently, the attention shifts towards optimizing the rear upright assembly, with the gathered insights to further enhance its performance while simultaneously reducing weight. The simulation of the rear upright was done differently than the front. This is due to the acceleration being the biggest force in the rear, in contrast to the front. The reason for this was previously discussed in more detail in Chapter 4.3.

All the connections to the frame are pin constrained in the same way as the simulation for the front upright. The previously calculated forces are.

$$V_{outer} = 2384\ N$$

$$H_{outer} = 2837\ N$$

$$V_{inner} = 1067\ N$$

$$H_{inner} = 1270\ N$$

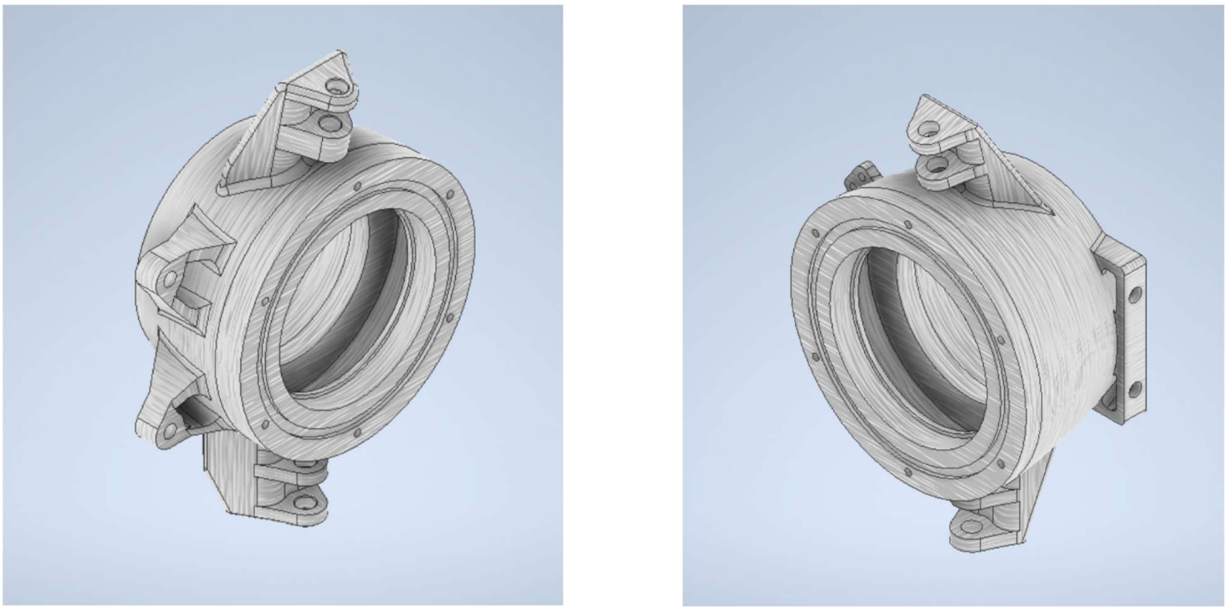

(a) *(b)*

Figure 5.3 illustrate updated and final upright designs of left front on the left in Figure (a) and left back to the right in Figure (b).

The main difference between the front and rear uprights is the different brake brackets, in addition to the separate places of the brackets where the car connects to the upright. Finally, a last simulation was performed on both parts to ensure that the forces had at least a safety factor of 1.2.

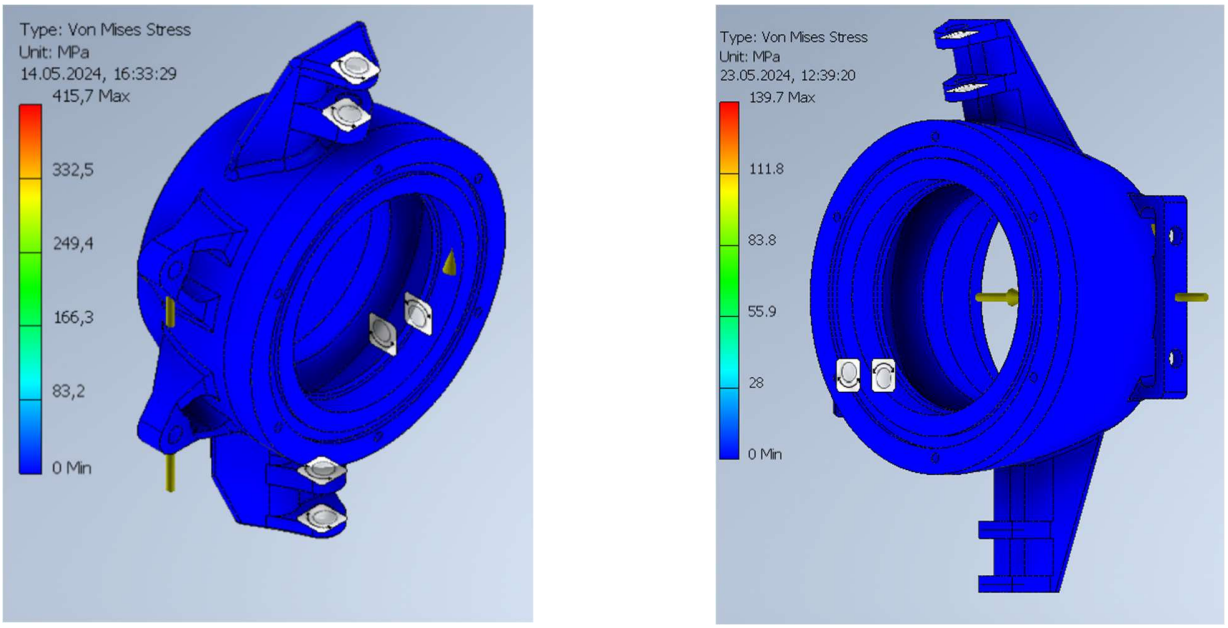

(a) *(b)*

Figure 5.4 illustrates the results from simulations on the final designs. Figure (a) is the left front up-right and (b) is the back left up-right. The yellow arrows represent the acting forces, and the white symbols represent where the pin constraints are.

These simulations shown in Figure 5.4 show that the stresses are within the safety factor. With safety factors of 1.2 and 3.5. The rear upright having a safety factor of 3.5 which is a lot bigger than the minimum of 1.2. In the further development of new uprights for ION Racing, it could therefore be made significantly lighter with a lower safety factor.

6. Discussion and further development

This project began with a series of requirements, divided into hard and soft categories. All the hard requirements were essential for the project's utilization and were, fortunately, all met—at least to current knowledge. The soft requirements are less directly measurable and can always be improved. The two soft requirements were:

- The design must be as future-proof as possible.
- The design must be lighter or the same weight as the previous generation.

Firstly, the future-proofness of the design is challenging to determine. The design aligns with ION Racing's vision and goal of converting to four-wheel drive. However, some design choices, such as the decision to make the camber angle fixed as shown in Figure 4.1.1, reduce flexibility. This decision was made to achieve the second goal of making the design lighter. It can therefore be argued that this design choice also contributes to future-proofing the design, making it the correct choice.

Another significant design decision was to opt for a simpler design rather than a complex one suitable for additive manufacturing. Although a design for additive manufacturing could potentially meet both soft requirements by being lighter and comparable in weight to the significantly smaller and less complex previous design, it might have compromised a more critical hard requirement. Due to higher complexity and costs, it might not have been feasible for ION Racing. This decision was therefore rightly deemed correct.

The design incorporates many of the same methods as previous ION Racing upright designs. One example is the method for removing unnecessary material, primarily by eliminating triangles due to their effective force distribution. While new and potentially more effective methods could be explored, their effectiveness is uncertain. ION Racing should investigate this further in the future, as it could significantly reduce weight.

Another approach to achieving weight reduction is to perform more accurate simulations. In this thesis, Autodesk Inventor stress simulation was used, but it was found to potentially exaggerate stresses. Additionally, identifying the exact locations of the highest stresses can be challenging, making it difficult to determine where to add or remove material. As a result, the process was more trial and error, a less optimal final design. However, it still provides a solid initial design for ION Racing's first four-wheel-drive race car. Perfecting the design is a continuous process, as there is always room for improvement. Since ION Racing has never had a four-wheel-drive car before, it will likely gather valuable information and knowledge as the project progresses.

7. Conclusion

One now has a design for new uprights, so ION Racing has the possibility of converting to four-wheel drive. However, the design is not perfect. This is a first design for ION Racing to make this conversion possible. This was also always the end goal of the project this thesis is a part of. The design has implemented several new features not used by ION Racing before with an improved upper arm bracket that is now lighter than previous designs. However, the design has also used what worked in previous designs, for instance by using the same method to reduce the weight.

The use of additive manufacturing methods were also discussed. This could possibly make the design significantly lighter due to the new design possibilities this leads to. However, this design proposal was rejected in this project due to the marginal benefits it offered in this context being deemed insufficient. It was instead decided to focus on a design that could be manufactured using traditional machining and manufacturing methods. This is one of the places ION Racing could gain the biggest weight reduction in the future, by using more advanced simulation methods based on finite element methods one could get a more accurate result which would make additive manufacturing beneficial. To conclude, the project still serves its purpose and opens up many possibilities for ION Racing, with the drawings for the final design provided in Appendices A and B.

References

If the source is not mentioned in the figure text, the figure is created by the author Mathias Alten.

asm.matweb. (2024, May 10). *7000 Series Aluminum Alloy*. Retrieved from asm.matweb: https://asm.matweb.com/search/SpecificMaterial.asp?bassnum=ma7075t6

asm.matweb. (2024, May 10). *7000 Series Aluminum Alloy*. Retrieved from asm.matweb: https://asm.matweb.com/search/SpecificMaterial.asp?bassnum=ma7075t6

Aune, P. A. (2016). *A Four Wheel Drive System for a Formula*. Trondheim: NTNU.

Autodesk. (2024, March 27). *CAD design*. Retrieved from Autodesk: https://www.autodesk.com/solutions/cad-design

Autodesk Inventor. (2024, May 8). *About Shape Generator*. Retrieved from Autodesk Inventor: https://help.autodesk.com/view/INVNTOR/2023/ENU/?guid=GUID-D74F47F3-FE22-44EF-85BE-7C6B1F56DCF9

Bhosale, D. A. (2024, May 7). *Unit II Vehicle Suspension Systems*. Retrieved from Govt. College of Engineering and Research, Avsari: https://www.gcoeara.ac.in/learning_material/auto/Unit%202-AST.pdf

Edurev. (2024, May 14). *Permissible Bending Stress in Steel*. Retrieved from Edurev: https://edurev.in/question/2814110/The-permissible-bending-stress-in-steel-is-a-1500kgcm2b-1890kgcm2c-1900kgcm2d-1300kgcm2Correct-answe

Engineers edge. (2024, May 5). *Yield Strength*. Retrieved from Engineers edge: https://www.engineersedge.com/material_science/yield_strength.htm

Ernst, L. (2024, May 15). *9+ Polar Moment Of Inertia Formulas [2024]*. Retrieved from structuralbasics.com: https://www.structuralbasics.com/polar-moment-of-inertia-formulas/

grabcad.com. (2024, March 12). *Front Suspension Design - UCL Formula Student*. Retrieved from grabcad.com: https://grabcad.com/library/front-suspension-design-ucl-formula-student-1

In3dtec. (2024, March 10). *Exploring The Difference: Metal 3D Printing Vs CNC Machining*. Retrieved from In3dtec: https://www.in3dtec.com/metal-3d-printing-vs-cnc-machining/

Ingham, D. R. (2024, March 13). *Car diagram*. Retrieved from Wikipedia: https://en.wikipedia.org/wiki/Unsprung_mass

Krönke, M. (2024, March 15). *Camber & Toe*. Retrieved from virtualracingschool: https://virtualracingschool.com/academy/iracing-career-guide/setups/camber-toe/

letstalkscience. (2024, May 22). *Why is a Triangle a Strong Shape?* Retrieved from letstalkscience: https://letstalkscience.ca/educational-resources/backgrounders/why-a-triangle-a-strong-shape

Massobrio, A. (2024, May 9). *What Is Meshing: Unlocking the Power of 3D Geometry*. Retrieved from neuralconcept: https://www.neuralconcept.com/post/what-is-meshing-unlocking-the-power-of-3d-geometry

Nafems. (2024, May 21). *The Importance of Mesh Convergence*. Retrieved from Nafems.org: https://www.nafems.org/publications/knowledge-base/the-importance-of-mesh-convergence-part-1/

Seward, D. (2022). *Race car design.* London: Bloomsbury Academic.

Team Xometry. (2024, May 10). *Yield Strength: Definition, Importance, Graphs, and How to Calculate*. Retrieved from Xometry: https://www.xometry.com/resources/3d-printing/yield-strength/

Tsyauto. (2024, May 14). *The Comprehensive Guide to Selecting the Ultimate Control Arms for Your Vehicle*. Retrieved from tsyauto: https://tsyauto.com/the-comprehensive-guide-to-selecting-the-ultimate-control-arms-for-your-vehicle/

Ulrich, K. T., Eppinger, S. D., & Yang, M. C. (2020). Product Design and Development. New York: McGrew-Hill Education.

Valor Offroad. (2024, March 13). *UNSPRUNG VS SPRUNG WEIGHT*. Retrieved from Valor Offroad: https://www.valoroffroad.com/blogs/the-source/how-wheel-weight-impacts-your-vehicle

Vedantu. (2024, May 18). *Introduction to Moment of Inertia*. Retrieved from Vedantu: https://www.vedantu.com/jee-main/physics-moment-of-inertia-of-a-square

Appendix

Appendix A

Drawing of front left upright.

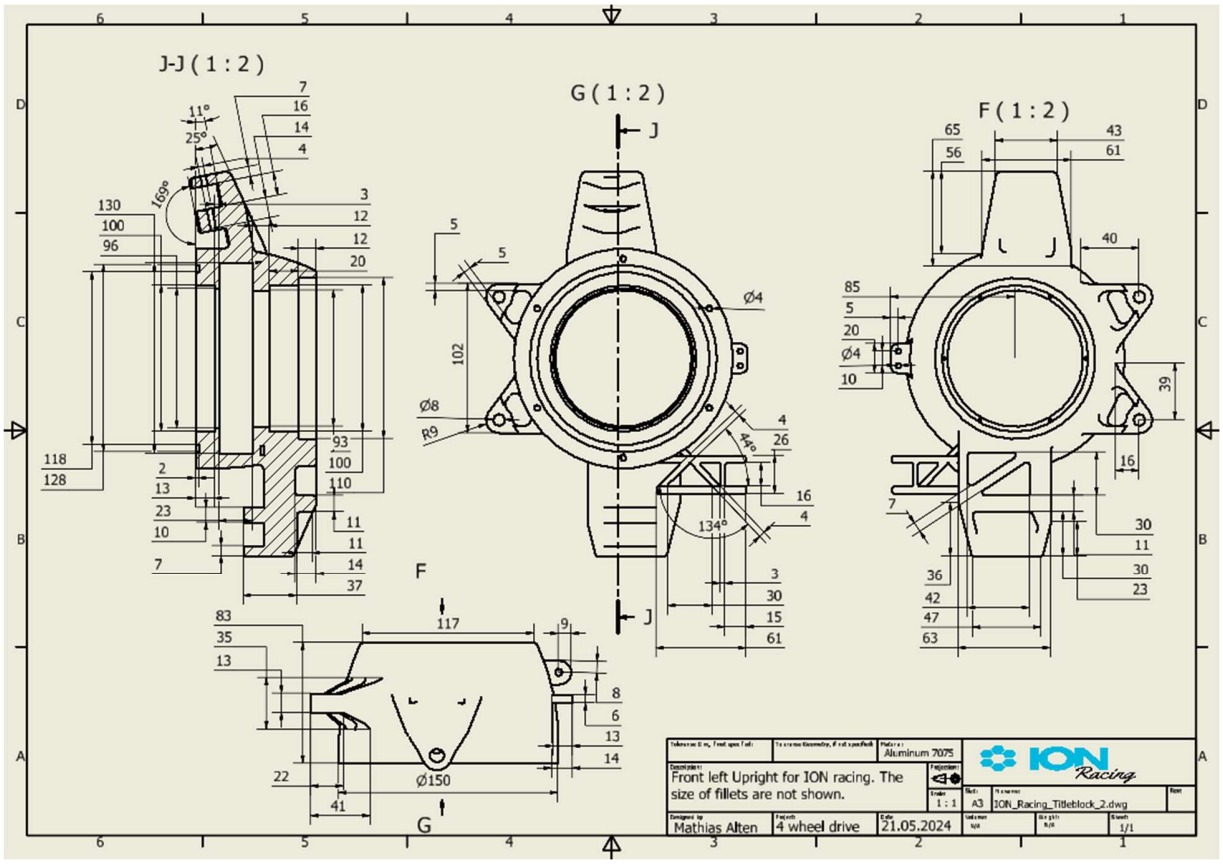

Appendix B

Drawing of back left upright.

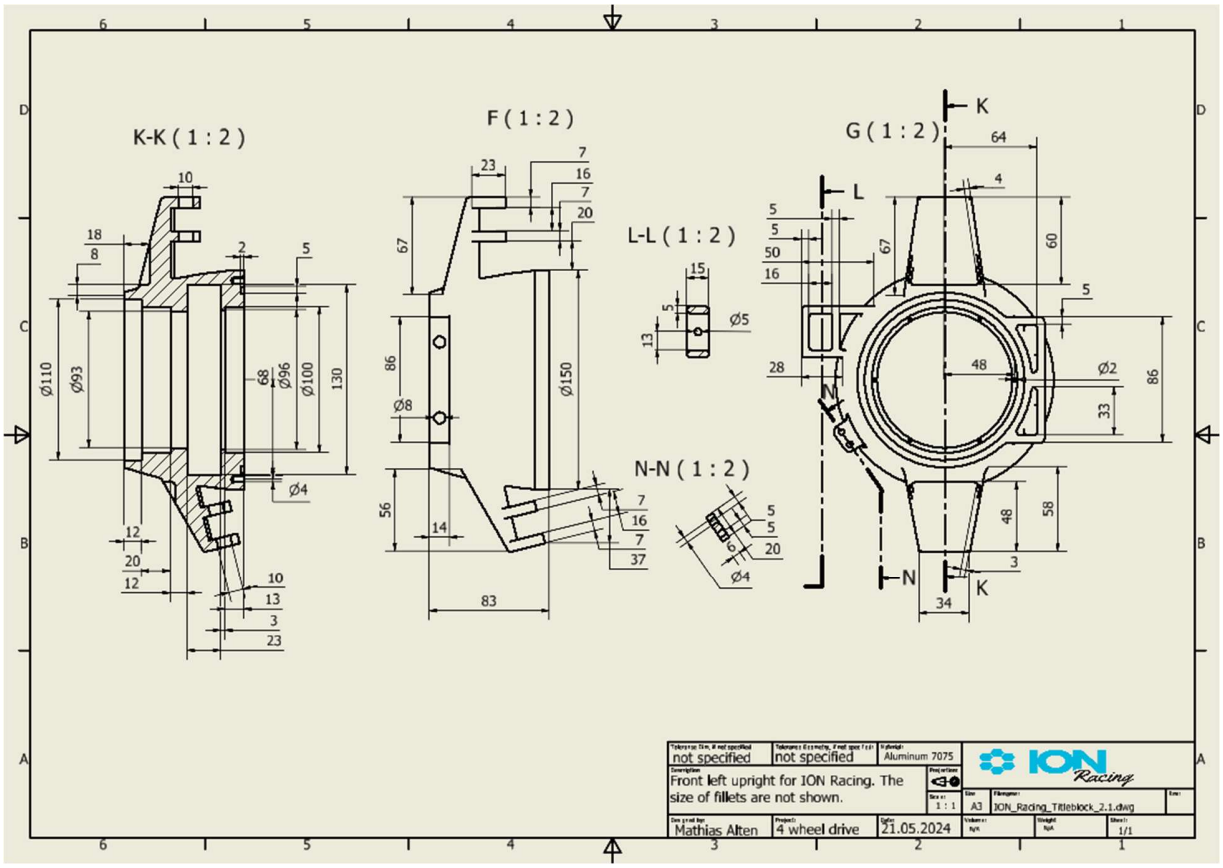

Appendix C

Tables with final points for the brackets on the upright.

Front:

	Point Name	Left		
		X	Y	Z
Double A-Arm	CHAS_LowFor	152.315	216.680	170.413
	CHAS_LowAft	-131.396	219.774	177.200
	CHAS_UppFor	139.369	265.086	320.000
	CHAS_UppAft	-122.423	267.015	320.000
	UPRI_LowPnt	5.000	549.000	140.000
	UPRI_UppPnt	-8.000	522.000	370.000
	CHAS_TiePnt	129.230	200.000	197.000
	UPRI_TiePnt	75.230	573.000	180.600

Rear:

	Point Name	Left		
		X	Y	Z
Double A-Arm	CHAS_LowFor	208.435	304.174	200.000
	CHAS_LowAft	-75.892	271.168	176.597
	CHAS_UppFor	193.310	326.179	311.117
	CHAS_UppAft	-68.883	308.583	311.117
	UPRI_LowPnt	0.000	547.000	150.000
	UPRI_UppPnt	0.000	522.000	360.000
	CHAS_TiePnt	-84.579	294.883	227.000
	UPRI_TiePnt	-85.000	550.000	227.000